INCORPORATION OF FLUORESCENT ANALOGUES IN ISOPRENOID PATHWAYS IN *ESCHERICHIA COLI*

by

Chelsea George

A thesis submitted to the faculty of
The University of North Carolina at Charlotte
in partial fulfillment of the requirements
for the degree of Master of Science in
Chemistry

Charlotte

2018

Approved by:

_____
Dr. Jerry Troutman

_____
Dr. Kirill Afonin

_____
Dr. Juan Vivero-Escoto

_____
Dr. Todd Steck

ABSTRACT

CHELSEA GEORGE. Incorporation of fluorescent analogues in isoprenoid pathways in *Escherichia coli*. (Under the direction of DR. JERRY TROUTMAN)

Bacterial glycans and glycoconjugates have wide diversity compared to their eukaryotic counterparts. While methods have been developed to monitor and track glycans in eukaryotic systems with some success, there are limited methods with which to do so in prokaryotes. Work conducted by Bertozzi has utilized alkyne-tagged sugars that, once incorporated into enzymatic pathways, can be clicked to a fluorophore for characterization.[1] However, due to the increased number of available sugars and potential combinations, this approach this approach becomes challenging in bacteria. Isoprenoids are one of the largest groups of naturally occurring compounds and are essential in all living organisms.[2] They are constituted of the building block isopentenyl diphosphate (IPP) and, in prokaryotes, are vital for nearly all polysaccharide biosynthetic pathways via the formation of the anchor bactoprenyl phosphate (BP).[3] This anchor is utilized in the cell membrane for a variety of biosynthetic pathways including those related to peptidoglycan (PG), capsular polysaccharides (CPS), exopolysaccharides (EPS), and others.[4] This work examines utilizing an exogenously introduced fluorescent isoprenoid to tag and monitor the formation of glycan intermediates in *Escherichia coli*. This approach has applications in identifying the functions of pertinent enzymes in previously unexamined pathways as well as better understanding associated glycan intermediates. The presented research discusses preliminary methods for incorporation of fluorescent compounds as well as several applications.

TABLE OF CONTENTS

LIST OF ABBREVIATIONS vii

LIST OF FIGURES viii

LIST OF TABLES x

CHAPTER ONE: INTRODUCTION 1

1.2: Isoprenoids in Glycobiology 1

1.3: Isoprenoids in Bacteria 4

1.3.2: General Biosynthesis of Polysaccharides in Bacteria 6

1.4: Isolation of Isoprenoid-Linked Sugars 7

1.5: Tracking Cellular Glycan Formation and Characterization 8

1.6: Methods to Permeabilize Bacterial Cells 10

1.7: Summary of Thesis Project 13

CHAPTER TWO: METHODS 18

2.1: Minimum Inhibitory Concentrations of Antibiotics and Other Compounds on *E. coli* 18

2.1.2: Statistical Analysis 19

2.2: Rescue of *E. coli* from Fosmidomycin 19

2.2.1. Kinetics of Fosmidomycin via ^{1}HNMR 20

2.3: Cellular Incorporation of 2CNA-GOH and 2CNA-GPP 20

2.3.1: Concentration Variation of 2CNA-GOH 21

2.4: Toxicity Assay of Fluorescent Farnesyl Diphosphate Analogues 21

2.5: Incorporation of Membrane Permeability Agents 22

2.5.1: Concentration Variation of PMBN 22

2.6: Time Point Labeling 23

2.6.1: Cellular Labeling over 24 h 23

2.6.2: 1 h Incubation of Cells with Fluorescent Analogues 23

2.7: Lysate Labeling 23
2.8: Characterization of Fluorescent Products 24
2.9.1: Separation and Analysis of Cellular Fractions 24
2.9.2: Isolation 25
2.9.3: Mass Spectrometry 25
CHAPTER THREE: DATA & RESULTS 27
3.1: Cellular Uptake of Isoprenoids is Possible 27
3.1.1: Rescue of *E. coli* from Fosmidomycin 27
3.1.2: ^{1}HNMR Fosmidomycin Kinetics 32
3.1.3: Farnesyl Diphosphate and Fluorescent Analogues Vary in Rescue Capabilities 34
3.1.4: Fluorescent Farnesyl Diphosphate Analogues are Toxic at High Concentrations 40
3.2: Cellular Incorporation of 2CNA-GOH and 2CNA-GPP 45
3.2.2: EDTA and PMB Impacts on Membrane Permeability 49
3.2.3: PMBN Assists with Membrane Permeation 55
3.2.4: Cellular Labeling of Isoprenoid-Linked Pathways Improves over Time 59
3.3: Verification of Analogue Uptake 62
3.4: Characterization of Fluorescent Products 70
3.4.1: Separation and Analysis of Cellular Fractions 70
3.4.2: Mass Spectrometry of Isolated Products 72
CHAPTER FOUR: DISCUSSION & FUTURE DIRECTIONS 74
4.1: Overview of Presented Research 74
4.2: Characterization of Isoprenoid-Linked Compounds 76
4.3: Applications of Fluorescently-Labeled Isoprenoids 77
4.3.2: Application of Presented Methods toward Genetic Mutants 78

4.3.3: Application of Presented Methods toward Protein Identification 79

REFERENCES 82

LIST OF ABBREVIATIONS

2CNA-GOH	Fluorescent FOH analogue
2CNA-GPP	Fluorescent FPP analogue
BP	Bactoprenyl monophosphate
BPP	Bactoprenyl diphosphate
CA	Colanic acid
Cam	Chloramphenicol
EDTA	Ethylenediaminetetraacetic acid
FLU	Arbitrary fluorescence units
FOH	Farnesol
Fos	Fosmidomycin
FPP	Farnesyl diphosphate
HPLC	High Performance Liquid Chromatography
IPP	Isopentenyl diphosphate
IPTG	Isopropyl β-D-1-thiogalactopyranoside
LB	Luria-Bertani
MEP	Non-mevalonate pathway
MIC	Minimum inhibitory concentration
MVA	Mevalonate pathway
OPP	Octaprenyl diphosphate
PG	Peptidoglycan
PMB	Polymyxin B
PMBN	Polymyxin B nonapeptide
Rcf	Relative centrifugal force
TPC	Total protein content
UDP	Uridine diphosphate
UppS	Undecaprenyl pyrophosphate synthase

LIST OF FIGURES

Figure 1. Comparison of mevalonate and non-mevalonate pathways 3
Figure 2. Chemical structures of various quinones found in bacteria 4
Figure 3. Formation of BPP from FPP and IPP 5
Figure 4. General biosynthesis of polysaccharides in *E. coli* 7
Figure 5. Structures of fluorescent FPP analogues 11
Figure 6. Chemical structures of compounds selected for improving membrane permeability 13
Figure 7. Chromatograms of 2CNA-linked analogues and BPP standards 16
Figure 8. Conceptual depiction of rescue studies 28
Figure 9. MIC of fosmidomycin 29
Figure 10. Triplicate rescue of *E. coli* from fosmidomycin with IPP 31
Figure 11. Structure of the antibiotic fosmidomycin 32
Figure 12. Kinetics of fosmidomycin in D_2O 33
Figure 13. ^{1}HNMR of fosmidomycin in D_2O 34
Figure 14. Triplicate rescue of *E. coli* from fosmidomycin with IPP and FPP 37
Figure 15. Triplicate rescue of *E. coli* from fosmidomycin with IPP and 2CNA-GPP 38
Figure 16. Triplicate rescue of *E. coli* from fosmidomycin with IPP and 2CNA-GOH 39
Figure 17. Toxicity of 2CNA-GOH and 2CNA-GPP 41
Figure 18. Toxicity of 2CNA-GOH and 2CNA-GPP with PMBN 43
Figure 19. Statistics for toxicities of 2CNA-GOH and 2CNA-GPP 44
Figure 20. Conceptual methodology for cellular labeling 45
Figure 21. Comparisons of cellular incorporation of 2CNA-GOH and 2CNA-GPP 47
Figure 22. Comparisons of various concentrations of 2CNA-GOH 48

Figure 23. MIC curves of EDTA and PMB 51
Figure 24. HPLC comparison of cells treated with different concentrations of EDTA 52
Figure 25. HPLC comparison of cells treated with different concentrations of PMB 53
Figure 26. Growth curve of *E. coli* cells treated with PMBN 56
Figure 27. Comparison of cells treated with 2CNA-GPP or 2CNA-GOH with and without PMBN 57
Figure 28. Comparison of cells treated with 100 μM 2CNA-GOH and varying concentrations of PMBN 58
Figure 29. Comparison of cells treated with 100 μM 2CNA-GOH and varying concentrations of PMBN from 3 to 30 μg/mL 58
Figure 30. Time point study with 2CNA-GOH and PMBN 61
Figure 31. Chromatogram of cells incubated with 2CNA-GOH for one hour 62
Figure 32. General methods for verification of analogue uptake 63
Figure 33. MIC curves of chloramphenicol and PMB 65
Figure 34. Comparison of lysed cell material treated with fluorescent analogues 66
Figure 35. Comparison of dead cell material treated with fluorescent analogues 68
Figure 36. Comparison of "grown LB" treated with fluorescent analogues 70
Figure 37. Comparison of membrane and cytoplasmic components 71
Figure 38. MS of products isolated from cells treated with 2CNA-GOH and PMBN at 29 min 73
Figure 39. MS of products isolated from cells treated with 2CNA-GOH and PMBN at 31 min 73

LIST OF TABLES

Table 1. Compounds and selected concentrations for MIC testing 18
Table 2. Percent relative increases of samples treated with 2CNA-GOH 48
Table 3. Percent relative increases of samples treated with PMB 54
Table 4. Percent relative increases of samples treated with 0.1 or 1 mM EDTA 54
Table 5. Percent relative increases of samples treated with varying concentrations PMBN 59
Table 6. Integrations of HPLC peaks from lysate treated with fluorescent analogues 66
Table 7. Integrations of HPLC peaks from lysate dead cell material treated with fluorescent analogues 68
Table 8. Integrations of HPLC peaks from recovered LB supernatant treated with fluorescent analogues 70
Table 9. Integrations of peaks from HPLC examining tested cytosolic and membrane fractions 72

CHAPTER ONE: INTRODUCTION

Glycobiology is the study of the structure, biosynthesis, and biology of saccharides that are widely distributed in nature. As a field of study, glycobiology combines carbohydrate chemistry and biochemistry to focus on the cellular and molecular biology of glycans.[5] Glycans, as well as their conjugates, are compounds that include variable lengths of saccharides and are critical to living organisms.[6]

Glycans are capable of undergoing a variety of modifications, which enhances their diversity and frequently serves to mediate specific biological functions. Further, nearly every class of biomolecule can be found in a glycosylated form, adding to their complexity and ubiquity. These glycoconjugates occur when glycans covalently link to non-carbohydrate moieties and include N-glycans, O-glycans, glycophospholipids, glycoproteins, and several others, all of which have functions necessary for living organisms.[7] Some of these processes require the intervention of other forms of conjugates, such as those formed by isoprenoids and other lipid-like moieties. N-glycosylation, in particular, relies on oligosaccharide donation from a polyisoprenyl carrier lipid found in the cell.[8]

1.2: Isoprenoids in Glycobiology

Isoprenoids are one of the largest groups of natural compounds and are essential in all living organisms.[2] Comprised of repeating five carbon isoprene units, isoprenoids are found in organisms across the three domains of life.[9] They are formed from repeating chains of the building block isopentenyl diphosphate (IPP), which is generated by one of

two pathways (Figure 1); in eukaryotes, mitochondria, archaea, and some bacteria, IPP is formed by the mevalonate (MVA) pathway while most bacteria utilize the non-mevalonate (MEP) pathway.[2] In eukaryotes, isoprenoids are utilized as cholesterol, steroids, dolichol, and other necessary compounds. In prokaryotes, the extent of these compounds is not fully understood, however it is known that isoprenoids are vital for nearly all polysaccharide biosynthetic pathways and for the regeneration of peptidoglycan. In relation to glycobiology, isoprenoids are necessary and often used for protein glycosylation or polysaccharide biosynthesis. In humans, for example, mutations in genes known to contribute to N-linked glycosylation can result in congenital defects and muscular dystrophy[10,11]; in yeast, isoprenoid lipids have been implicated as necessary for the coordination of spore wall layers.[12]

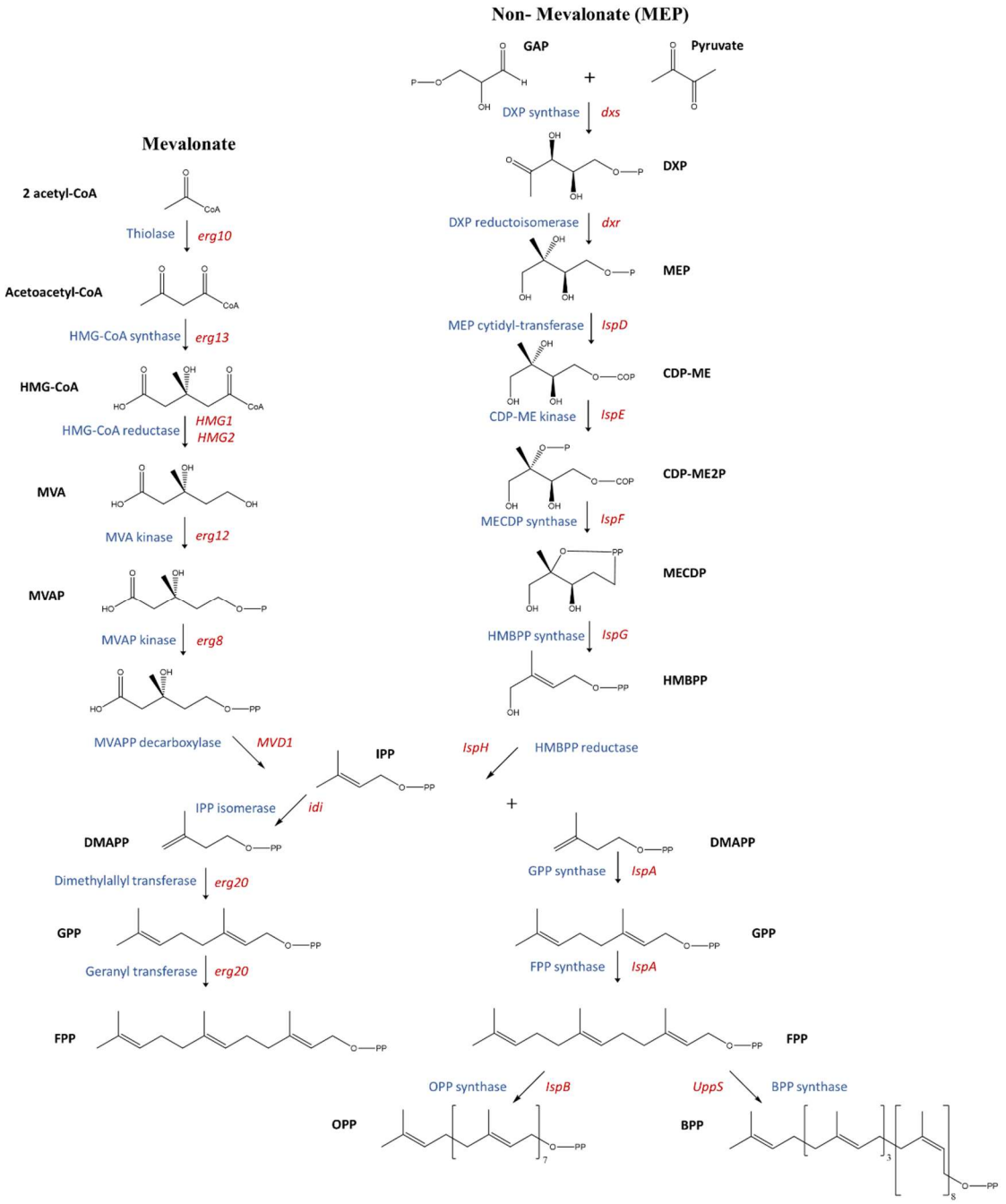

Figure 1. Comparison of mevalonate and non-mevalonate as well as isoprenoid biosynthetic pathways in eukaryotes and prokaryotes. The mevalonate pathway is utilized by eukaryotes exclusively, however some prokaryotes are capable of using both pathways. Adapted from Oldfield (2006).[13]

1.3: Isoprenoids in Bacteria

In bacteria, isoprenoids are abundant and may be found in the forms of carotenoids as well as plastoquinones and chlorophyll in photosynthetic bacteria (Figure 2). Further examples include compounds such as ubiquinone and menaquinone which are produced by several species of bacteria and are related to electron transfer.[14-16] These isoprenoid-linked quinones are typically associated with antioxidant function or electron transport, including photosynthetic activity.[17] The precursor for their side chains, octaprenyl diphosphate (OPP), is structurally similar to a larger compound associated with polysaccharide biosynthesis, bactoprenyl diphosphate (BPP), except in that it is three isoprene units shorter.

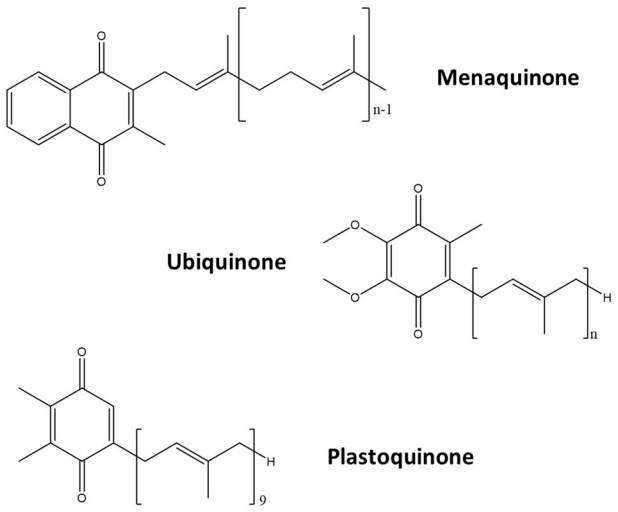

Figure 2. Chemical structures of various quinones found in bacteria. For menaquinone and ubiquinone, n is equal to the total number of isoprenoid units.

Isoprenoids have been shown to be especially vital to polysaccharide biosynthesis in the form of bactoprenyl phosphate (BP). The diphosphorylated version of BP is formed by undecaprenyl pyrophosphate synthase (UppS), an enzyme that combines

farnesyl diphosphate (FPP) and eight IPP units in sequential condensation reactions (Figure 3). The resulting BPP is cleaved by a phosphatase to yield BP. This is then utilized in the cell membrane as an anchor for a variety of biosynthetic pathways including those related to peptidoglycan (PG), capsular polysaccharides, exopolysaccharides, and other saccharides.[4] It has been believed that undecaprenyl pyrophosphate phosphatase (UppP) is responsible for the formation of BP from BPP, however some researchers suggest that UppP is utilized in the recycling of BP, not the formation.[18] Previously, it has been suggested that a kinase converts *de novo* bactoprenol to BP.[19-20] Recent research has not only reaffirmed the hypothesis for the formation of BP from BPP, but also identified other phosphatases, namely PgpB, YbjG and LpxT, that may play roles in either the production or recycling of BP.[21]

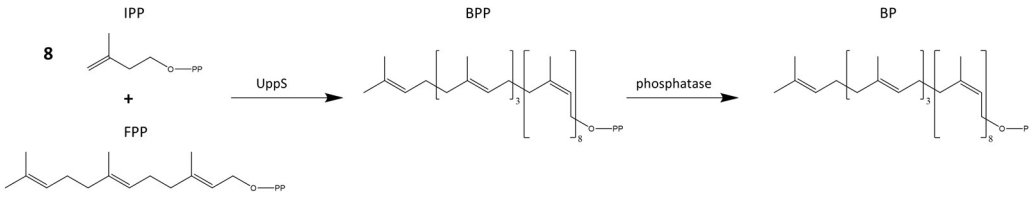

Figure 3. Formation of BPP from FPP and eight IPP molecules by successive condensation reactions via UppS. This is followed by a reaction with a phosphatase to yield the polysaccharide anchor, BP.

It is currently understood that most living organisms are capable of endogenously generating needed isoprenoids such as IPP and BP without uptake from the environment. However, research conducted by the Oldfield group has shown that bacterial cells are capable of utilizing exogenously acquired IPP under extreme duress.[22] Based on aspects of this research, it is hypothesized that fluorescently-labeled isoprenoid precursors could

be internalized and employed in order to track isoprenoid pathways; much of the presented work focuses on this approach. Further, it was hypothesized that exposing *E. coli* to stress-provoking conditions, such as antibiotics, influences isoprenoid production and could increase the success of internalization of exogenous isoprenoids. This series of experiments, termed "rescue studies" throughout the presented research, will be discussed in detail in a later section.

1.3.2: General Biosynthesis of Polysaccharides in Bacteria

As previously noted, polysaccharide biosynthesis in bacteria takes place utilizing BP as an anchor located in the membrane (Figure 4). BP first undergoes reaction with a phosphoglycosyl transferase. Several glycosyl transferases then transfer sugars in succession and modifications may occur such as acetylation. A flippase in the inner membrane flips the BPP-attached polysaccharide toward the periplasm where the polysaccharide is then polymerized. The full mechanism is not currently understood, but following polymerization, a transport system delivers the polysaccharide to the exterior portion of the membrane, and the BPP is left to be recycled for further use.

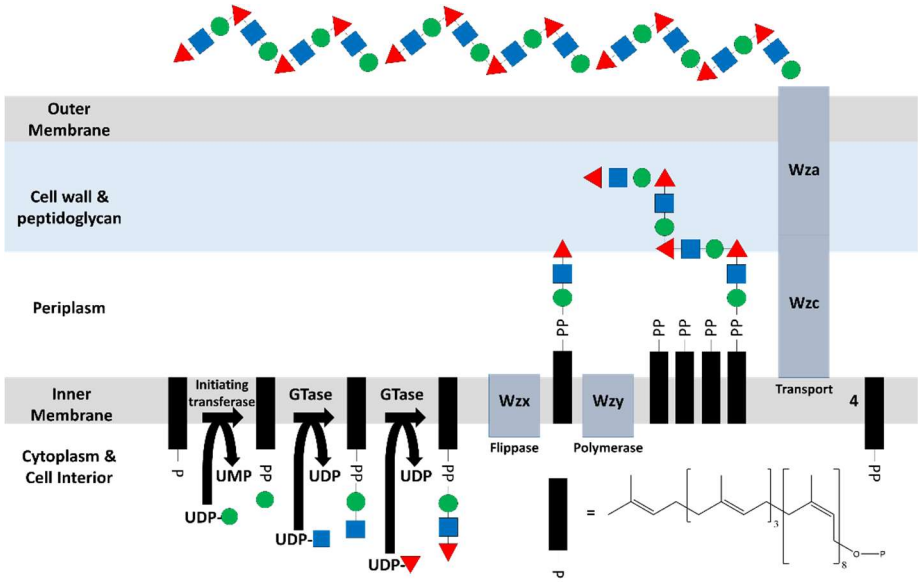

Figure 4. General biosynthesis of polysaccharides in *E. coli* utilizing a Wzy-dependent transporter pathway. Figure adapted from Whitfield[23] and created by J.M.Troutman

1.4: Isolation of Isoprenoid-Linked Sugars

The acquisition and characterization of polysaccharides and glycoconjugates is critical for the unraveling of their respective functions. However, obtaining these compounds from natural sources is often difficult due to the complexity of associated pathways.[24] Additionally, as these pathways are sometimes not yet elucidated, harvesting these compounds from natural sources is challenging. Approaches to study glycans and glycoconjugates often rely on one of two methods: chemical or enzymatic synthesis.

Chemical synthesis, while possible, is often challenging due to variables such as the reactivity of reagents and the need to modulate stereochemistry.[6] This becomes more difficult as the complexity of the desired glycan increases. For example, to synthesize capsular polysaccharide A, a tetrasaccharide associated with *Bacteriodes fragilis*, over 20 steps are required.[25] While this is quite an accomplishment, the biologically active polymer requires, at minimum, eight linked tetrasaccharide units.[26] Furthermore, being

unlinked to the isoprenoid limits use for the examination of associated enzymes such as transport proteins.[27]

Enzymatic synthesis can often make this process easier due to the inherent specificity commonly associated with enzymes. Bacterial glycosyltransferases, for example, can be readily mass-produced and purified. Some of these enzymes also exhibit a degree of promiscuity that enables the transfer of a wide array of sugars[28]; while this may create complications in one-pot reactions, this allows the use of alternate enzymes in the event that a desired glycosyltransferase is not easily expressed. Further, as shown with capsular polysaccharide A, functional polysaccharide units can be acquired in one-pot reactions.[27]

1.5: Tracking Cellular Glycan Formation and Characterization

Historically, approaches taken to study glycans mirrored those originally developed for proteins and nucleic acids. These approaches included disrupting structure or expression, defining physiological function, and attempts at visualization.[29] However, techniques for proteins and nucleic acids rarely translate well into glycan characterization; this is largely because a genomic template cannot direct glycan synthesis. This ultimately makes the elucidation of underlying molecular mechanisms that govern glycan function a substantial challenge. For example, while enzymes in metabolic pathways, such as glycosyltransferases, can be modified, the effects are not always clear and can result in unintentional or indirect lethality.[30-31] This undesired effect also occurs from perturbing glycan pathways associated with isoprenoids as shown by Young.[3-4, 32]

The majority of biosynthetic pathways that exist for the formation of capsular and exopolysaccharides utilize Wzy-dependent transporter pathways. The Troutman lab has worked extensively on the pathway associated with the exopolysaccharide colanic acid (CA) from *Escherichia coli*. The gene cluster for CA, known to use the Wzy-dependent system, has been identified, but the exact functions of the polysaccharide or the genes encoding it have not yet been determined. This is largely due to the innate difficulties that surround identifying repeating polysaccharide chains; when one gene is deleted in the sequence, the impacts are often difficult to identify or observe due to the full elimination of the repeating saccharide unit. For example, if a polymerase is silenced or removed from a glycan pathway, the complete polysaccharide cannot form; likewise if an earlier enzyme from the same pathway is removed, a similar result occurs. This limits the use of genetic knockouts for analysis of final glycan structures.

In recent years, efforts in fluorescently tagging cells has revealed valuable insights into these structures. In eukaryotes, azide-linked sugar residues have been successfully used in conjunction with fluorophores via copper-free click chemistry to study developmental stages of model organisms *in vivo*.[33] FPP analogues have also been used in eukaryotes where they interact with CaaX proteins via prenylation.[34] CaaX proteins assist in regulating a number of cellular signaling processes such as cell proliferation, differentiation, and metabolism, making them an attractive target for understanding these events in eukaryotes.[35] Once prenylated via this method, the protein can be visualized due to fluorescent moieties. However, these approaches have not been utilized in bacteria.

The Troutman lab has worked toward developing a powerful platform for the identification of proteins involved in glycan biosynthesis. This approach incorporates fluorescently-labeled isoprenoids in bacterial biosynthetic pathways and takes advantage of the multipurpose use of BPP in bacteria. This platform involves the use of anilinogeranyl diphosphate (A-GPP) linked to fluorescent moieties, of which many have been synthesized (Figure 5). The main benefits of utilizing labeled A-GPP are that it is a) analogous to FPP, a natural reagent for isoprenoid biosynthesis, and b) an acceptable substrate for UppS.[36] Once elongated, the formed product is a tagged anilinobactoprenyl diphosphate (A-BPP). Due to the fluorescent nature, this product is easily detectable and quantifiable via high performance liquid chromatography (HPLC). The hidden power of this approach is the versatility that comes with the use of different aniline substituents; highly fluorescent substituents are beneficial for low detection limits, some have improved solvatochromic properties and others are easily synthesized, allowing for the use of higher concentrations and therefore larger yields of labeled products. Analogues containing an azide moiety have also been synthesized to undergo "click chemistry" with strongly fluorescent compounds for improved visualization.

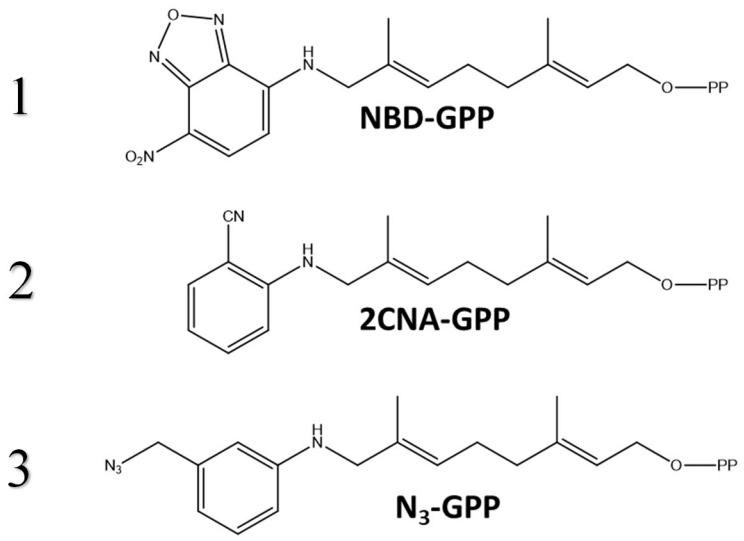

Figure 5. Structures of fluorescent analogues, including 2CNA-GPP, nitrobenzofurazan (NBD) GPP, and an azide GPP. All three analogues have separate value: 1) 2CNA-GPP is a smaller analogue and interacts well with UppS, 2) NBD-GPP has improved fluorescence and can be visualized in the visible spectrum, and 3) N_3-GPP has the ability for other chromophores to be "clicked" onto it, improving visibility of desired compounds.

1.6: Methods to Permeabilize Bacterial Cells

While enzymatic studies have shown success utilizing our fluorescent analogues, *in vivo* studies required considerations such as membrane permeability and analogue uptake. It was hypothesized that a FPP analogue would be less capable of permeating the double membrane of a Gram negative bacteria without active uptake due to its charged nature. Research in mammalian cells has shown that some enzymes are capable of utilizing farnesol analogues in place of FPP.[37] Based on this as well as the diphosphate charge consideration, it was further hypothesized that an alcohol rather than a diphosphate moiety on the analogue might assist with uptake. In order to assist with uptake of isoprenoid precursors, membrane permeabilization techniques were utilized, the outcomes of which will be discussed later.

Cellular membranes are typically permeabilized in order to improve uptake of a given material such as nutrients, drug delivery systems, or nucleic acids. In mammalian cells, drug delivery systems often focus on the endocytosis pathways, though bacteria are not thought to employ this approach. However, the Gram negative bacteria *Gemmata obscuriglobus* has been found to utilize a pathway analogous to endocytosis, showing that this form of uptake may be possible in certain species.[38] To encourage the uptake of genetic material during bacterial transformation, cellular membranes are intentionally compromised either by chemical competency or electroporation. Other methods utilized to permeabilize cell membranes include the use of chelating agents such as EDTA or antibiotics that interact with some portion of the cell membrane. EDTA functions to interact with Mg^{2+} and Ca^{2+} in the membrane, which results in a disruption of the lipopolysaccharide (LPS). This disruption compromises the ability to prevent passive diffusion of certain compounds, thereby increasing permeability.[39-40] Antibiotics such as polymyxin B sulfate (PMB) rely on a dual-action approach that involves the interaction of a fatty acid moiety with the outer membrane, thereby disrupting it; once permeation occurs, the antibiotic can interact with the cytoplasmic membrane causing further disruption.[41] Derivatives such as polymyxin B nonapeptide (PMBN), which lacks the fatty acid portion of the compound, display similar permeabilizing action, however are less bactericidal and do not appear to interact with the cytoplasmic membrane.[40, 42] The lack of a lethal action therefore makes PMBN an ideal candidate for assisting with permeation without compromising cell survivability. The structures of these three

compounds are shown in Figure 6.

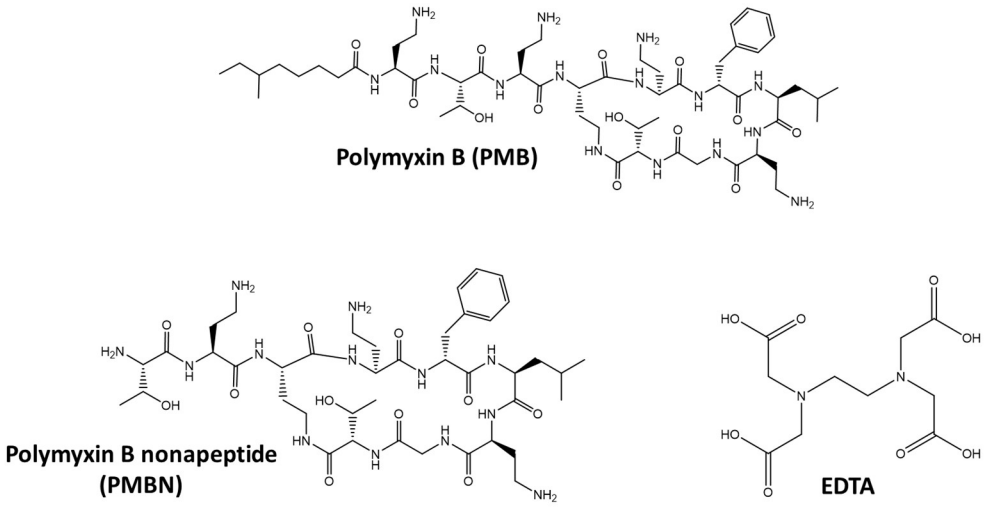

Figure 6. Chemical structures of compounds selected for improving membrane permeability.

Genetic mutants have also been examined for their potential uptake of isoprenoids. Five Tlc translocases found in *Rickettsia prowazekii*, for example, are known to be involved with the uptake of environmental materials. To date, only Tlc1, Tlc4, and Tlc5 have identified functions; Tlc1 transports ATP and ADP while Tlc4 and Tlc5 transport ribonucleotides for nucleic acid biosynthesis.[43]

Most bacteria are capable of generating their own isoprenoids via either the mevalonate or non-mevalonate pathway (Figure 1), but *Rickettsia* lacks the enzymes required for these pathways. However, enzymes involved in later isoprenoid biosynthesis such as UppS are conserved. This indicates that this genus of bacteria requires uptake of exogenously-acquired isoprenoids to generate vital compounds such as those associated with electron transport.[44] Based on this past research, it is hypothesized that either Tlc2 or Tlc3 may be involved with isoprenoid uptake.

1.7: Summary of Thesis Project

Glycans are ubiquitous and essential to all organisms. Researchers have uncovered several roles for glycans including cell development, organization, host-pathogen interactions, and immune responses.[45] However, due to discrepancies between the elucidations of glycan pathways compared to those associated with protein and nucleic acids, new strategies to understand these pathways are required. Former techniques to track glycan pathways in eukaryotes have often focused on the utilization of chemically-modified sugars.[46] Prokaryotes harness the metabolic capacity to incorporate and modify a larger array of sugars than eukaryotes do, which makes this approach challenging. Therefore, this research proposes a new approach in bacteria, focused on monitoring glycan biosynthesis via linked isoprenoids.

The first aim of this project is to establish a method to produce fluorescently labeled isoprenoid products from *E. coli* cells during growth. Fluorescent FPP analogues will be utilized alongside their alcohol variants. As mentioned, FPP analogues have been used in eukaryotic systems previously for the visualization of select proteins.[47] Past research from the Troutman lab has had success utilizing 2CNA-GPP as well as other FPP analogues in enzymatic reactions with UppS.[36, 48-49] It is therefore anticipated that the fluorescent analogues will be capable of undergoing incorporation into isoprenoid pathways and ultimately lead to the formation of tagged BP for visualization of linked sugars.

Proper analogue selection and concentration will both be necessary for the success of this project. In the Troutman lab, we have had the most reliable results from

compounds such as 2CNA-GPP. We believe this success may be due to the relatively small size of the fluorescent moiety in comparison with other available analogues. Based on this, as well as efforts from other members of the lab (data not presented), we have decided to primarily utilize the 2-nitrile compounds. As for concentration, we anticipate that only a portion of the analogue may pass through the cell membrane; it is currently uncertain if or how large an excess of analogue is needed. This will be tuned according to preliminary results. Other parameters such as growth time, lysis conditions, and the addition of a membrane permeabilizer will be examined in a systematic manner with the goal of optimizing labeled product formation as visualized by HPLC.

Once a successful method is established for labeling isoprenoids in bacterial cells, the second aim is to characterize products via mass spectrometry (MS), enzyme reactions, and comparison to standards. It has been previously demonstrated that we are capable of modulating the length of bactoprenyl products using select detergents.[36] Using this technique and MS verification, we have compiled standards with expected HPLC retention times that will be compared to labeled products (Figure 7). Based on this, we will be able to hypothesize the identities of potential products. These products can then be reacted with appropriate enzymes; if expected changes are observed relative to controls, we will interpret this as supporting evidence toward our hypotheses of the identification of the products. Finally, we will isolate fluorescent products via HPLC and analyze them via MS. We anticipate that these combined approaches will begin the characterization process for these materials.

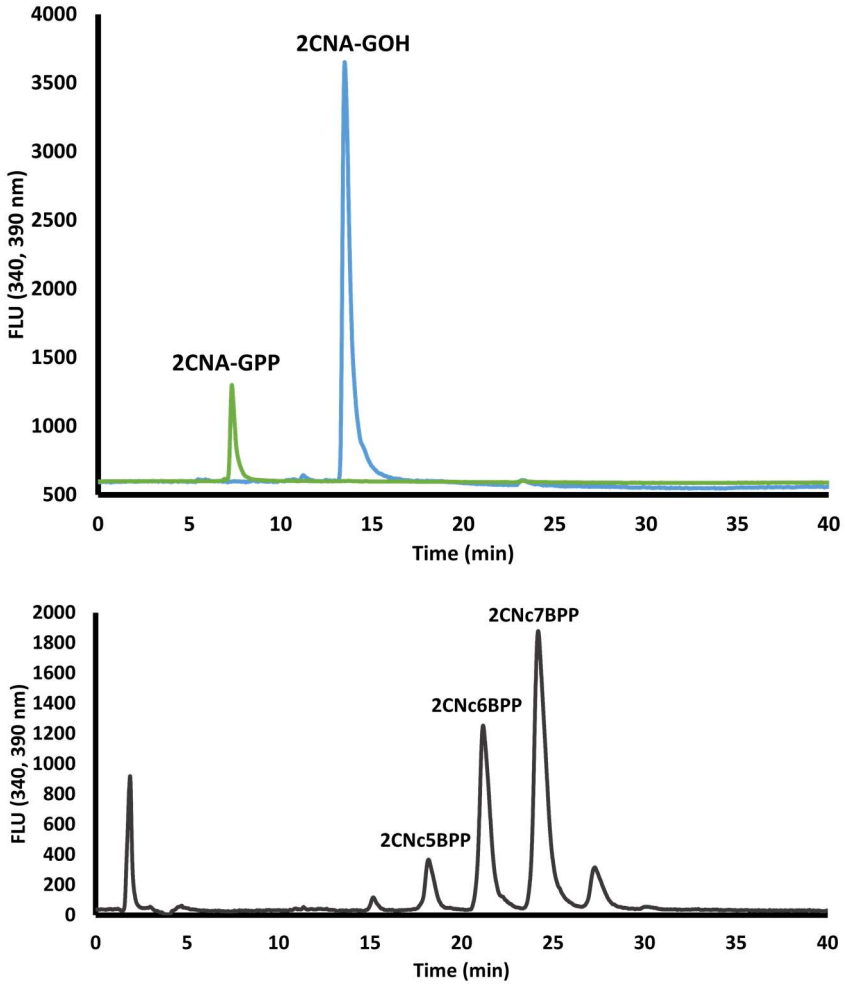

Figure 7. Chromatograms of 2CNA-linked analogues and BPP standards depicting retention times using a *n*-PrOH gradient and monitoring fluorescence.

This research also explores the capacity to differentiate isoprenoid-linked glycan intermediates in a given pathway. We will focus on utilizing genetic knockouts from the CA pathway to meet this end. As each knockout should result in a buildup of a unique intermediate, we anticipate the observation of distinct differences via HPLC. There is the possibility, however, that these products may display similar retention times, which may prove problematic. For this, HPLC method development may prove useful as well as MS to detect separate products.

Finally, this research begins to examine the functions of the Tlc2 and Tlc3 proteins that naturally occur in *Rickettsia prowazekii*. This is accomplished by comparing the uptake capacity of 2CNA-GPP relative to each other, as well as a control. Presumably, if either is capable of amplifying isoprenoid uptake, a noticeable difference will be seen. While this research does not conclusively determine the absolute function of either protein, it does indicate that one is more likely associated with isoprenoid uptake compared to the other. Further work will be required for this and is discussed in Chapter 4.

CHAPTER TWO: METHODS

2.1: MICs of Antibiotics and Other Compounds on *E. coli*

A minimum inhibitory concentration (MIC) was conducted on *E. coli* strain MAJ427, acquired from the University of Arkansas. MAJ427 is a variant of wild type MG1655 with a repaired O-antigen and kanamycin resistance. The minimum inhibitory concentrations (MIC) were conducted in a 96-well plate with PMB, PMBN, carbenicillin, chloramphenicol, fosmidomycin, and EDTA, based on a published protocol.[50]

Table 1. Compounds and selected concentrations for MIC testing of MAJ427, all of which were diluted in LB with kanamycin from stock solutions.

Antibiotic or compound	Tested concentrations
Polymyxin B (PMB)	0.001, 0.01, 0.05, 0.07, 0.1, 1, 10 µg/mL
Polymyxin B nonapeptide (PMBN)	10, 20, 30, 40, 50 µg/mL
Chloramphenicol	0.05, 0.5, 5, 10, 20, 25, 50 µg/mL
Fosmidomycin	0.001, 0.01, 0.1, 1, 5, 10, 50 µM
EDTA	0.01, 0.1, 1, 5, 7, 10, 50 mM

A starter culture from a glycerol stock was grown overnight and then plated. Isolated colonies were picked and grown to an OD_{600} of 0.6 in LB with 50 µg/mL kanamycin (kan^{50}) which was then diluted 1:100. Experimental wells were inoculated with 10 µL of the diluted cells and brought to a final volume of 100 µL per well. Samples were grown for 120 cycles at 37 °C on a Fluostar Galaxy plate reader, taking absorbance measurements every 600 s and shaking at a rotation width of 6 mm for 300 s per cycle. For this purpose, a cycle represents a single data point and lasts for 600 s. Shaking occurred for half of each cycle.

2.1.2: Statistical Analysis

Statistical analysis for all MICs was conducted on the software GraphPad. A Gompertz fit was applied to the data as described by Lambert and Pearson.[51] This fit is a mathematical model which describes growth as being slowest at the start and end of a given time period.

2.2: Rescue of *E. coli* from Fosmidomycin

"Rescue" experiments have been previously reported by Oldfield.[22] Fosmidomycin was utilized for its ability to inhibit the non-mevalonate pathway and limit the amount of endogenous isopentenyl diphosphate (IPP) present. Cell cultures were prepared similarly to MIC experiments in section 2.1. Based on results from the previously mentioned MIC experiment, fosmidomycin 10 μM was chosen as the preferred inhibitory concentration. Fosmidomycin and IPP were prepared from stock solutions and diluted to 0.1, 0.5, 1, 5, and 10 mM, respectively, in LB with kan[50]. In a 96-well plate, experimental wells were inoculated with 10 μL of the diluted cells and brought to a final volume of 100 μL per well. 10 μL of fosmidomycin and IPP solutions were added to appropriate wells using a multichannel pipette to final concentrations of 10 μM and 0.05, 0.1, 0.5, and 1 mM, respectively. Samples were grown on a Fluostar Galaxy, as mentioned previously in section 2.1.

Based on the experiment above, a concentration of 1 mM IPP was chosen for rescue in conjunction with 2CNA-GPP, 2CNA-GOH, or FPP. To accomplish this, cell cultures were prepared as mentioned previously in section 2.1 with 10 μM

fosmidomycin, 1 mM IPP, and a gradient of analogue ranging from 5 to 250 µM. PMBN was also added at a final concentration of 15 µg/mL. Samples were grown in a Fluostar plate reader under the same conditions as above.

For statistical analysis, measured absorbance values from 18-20 h were averaged and plotted for each sample. Both f-tests and t-tests were conducted using Microsoft Excel for examination of statistical significance.

2.2.1. Kinetics of Fosmidomycin via ^{1}HNMR

25 mg of fosmidomycin was dissolved in 500 µL D_2O and analyzed on a JEOL 500 MHz NMR. The offset was set at 5 ppm and the sweep was set to7.5 kHz. Every hour, 8 scans were taken with a relaxation time of 5 s.

2.3: Cellular Incorporation of 2CNA-GOH and 2CNA-GPP

Starter cultures of MAJ427 were prepared from a glycerol stock and grown overnight in LB with kan^{50}. The culture was then diluted to an OD_{600} of 0.6-0.8 and 200 µL was added to a 5 mL culture of LB with kan^{50}. 2CNA-GOH in DMSO or 2CNA-GPP was added for a final concentration of 100 µM. Experimental, blank, and control cultures were shaken for 18 h at 37 °C on a New Brunswick Scientific shaker at 220 rpm. Following growth, 4.5 mL of cultures were centrifuged for 10 min at 3500 relative centrifugal force (rcf) and the LB supernatant was removed and saved for analysis. Pellets were washed in 1 mL of 0.9% NaCl and centrifuged for 15 min at 19,750 rcf at room temperature; this process was repeated for a total of 2 washes. Washed pellets were suspended in 500 µL of lysis buffer (50 mM Tris, 50 mM NaCl, 0.1% Triton) and

sonicated for 2 min on ice at 25% amplitude pulsing 1 s on, 2 s off using a Fisher Scientific Model 500 Ultrasonic Dismembrator. Total protein concentration from cell lysate for normalizing cell content was analyzed in a 96-well plate following a BIORAD Bradford microassay protocol.[52] Total protein content was adjusted based on the lowest concentrated sample; all other samples were diluted in lysis buffer to appropriate concentrations. Samples were then filtered with a 0.2 μm polyethylene filter in preparation for HPLC analysis. HPLC analysis was performed on an Agilent 1100 HPLC instrument equipped with an autosampler, a diode array detector, a fluorescence detector, and an inline degasser. The HPLC stationary phase was a reverse phase c18 Agilent Eclipse XDB-c18, 5 μm, 4.6 mm × 150 mm column. The mobile phase consisted of 100 mM ammonium bicarbonate and variable amounts of *n*-propanol starting at 15% and increasing to 95% over 36.9 min. Nitrileaniline-linked analogues were monitored by fluorescence at an excitation wavelength of 340 nm and an emission wavelength of 390 nm.[36]

2.3.1: Concentration Variation of Fluorescent Analogues

Cells were prepared and treated as mentioned in section 2.3. Concentrations of 2CNA-GOH were further varied to 10, 25, 50, and 100 μM for comparison. Once grown for 18 h, cells were lysed and prepped for HPLC analysis.

2.4: Toxicity Assay of Fluorescent FPP Analogues

Toxicity of 2CNA-GOH and 2CNA-GPP was measured by absorbance via plate reader, with a similar protocol as mentioned previously in section 2.1. Cells were

prepared as in section 2.1 and experimental wells in a 96-well plate were inoculated with 10 µL of cells. Fluorescent analogues were analyzed in final concentrations of 0, 50, 100, 250, 500, 750, and 1000 µM. Total volumes were brought to 100 µL and cells were grown in a Fluostar plate reader as described previously.

For statistical analysis, measured absorbance values from 18-20 h were averaged and plotted for each sample. Both f-tests and t-tests were conducted using Microsoft Excel for examination of statistical significance.

2.5: Incorporation of Membrane Permeability Agents

To improve analogue uptake, cells were grown as previously mentioned in section 2.3 with 100 µM 2CNA-GOH and in the presence of PMB, PMBN, or EDTA. Gradients were first analyzed to establish usable concentrations, and 0.1 µg/mL PMB, and 10 mM EDTA were chosen for further examination. For PMBN, 15 and 30 µg/mL demonstrated similar success, however 15 µg/mL was chosen for future experiments (section 2.5.1). Following sonication, samples were matched based on total protein content (TPC) via a Bradford microplate assay in a clear 96-well plate. Samples were filtered, diluted in lysis buffer to similar concentrations, and analyzed via HPLC.

2.5.1: Concentration Variation of PMBN

Concentrations of PMBN of 0.3, 3, and 30 µg/mL were tested in conjunction with 100 µM 2CNA-GOH as laid out in sections 2.3 and 2.5. After analysis, concentrations of 3, 10, 15, 20, and 30 µg/mL PMBN were further tested and analyzed via HPLC.

2.6: Time Point Labeling

2.6.1: Cellular Labeling over 24 h

MAJ427 cells were prepared as mentioned previously in section 2.3. To ensure consistency for culture preparation, a total of 40 mL LB with kan^{50} was inoculated with 1.6 mL of the diluted cells. Of this mixture, 5 mL was removed for a control and the remaining media was treated with 100 μM 2CNA-GOH and 30 μg/mL PMBN; this was then divided into seven identical cultures. The cultures were incubated at 37 °C and shaken for 4, 8, 12, 16, 18, 20, or 24 h; the control was allowed to grow for 24 h. Following growth, cultures were pelleted, washed, and prepped for HPLC analysis. For both alcohol and diphosphate samples, analytical HPLC was performed using a gradient method with a mobile phase of 100 mM ammonium bicarbonate (A) and *n*-propanol (B). The method started at 15% B and then increased to 95% B over 36.9 min.

2.6.2: 1 h Incubation of Cells with Fluorescent Analogues

A cell culture of MAJ427 was prepared as in section 2.3, however no fluorescent analogue was added until the 18 h mark during growth. Cells were allowed to incubate for another 1 h following inoculation and were compared to a control culture that had been labeled the full 18 h. HPLC analysis was conducted.

2.7: Lysate Labeling

An MIC was conducted in a 96-well plate (discussed previously in section 2.1). Following data analysis, 0.1 μg/mL PMB and 25 μg/mL chloramphenicol in conjunction were selected for future experiments.

A starter culture of MAJ427 was grown from a streak plate to an OD_{600} of 0.6 and diluted 1:100. This was then diluted 1:10 in 5 mL cultures of LB with kan^{50}, and the aforementioned concentrations of PMB and chloramphenicol. The cultures were shaken overnight at 37 °C and plated to ensure no further growth had occurred. The "dead" cultures were inoculated with 2CNA-GOH or 2CNA-GPP and shaken another 18 h at 37 °C with labeled cell cultures as control.

In another approach, 5 mL cultures of MAJ427 were grown in LB with kan^{50} for 18 h and pelleted. The supernatant was removed and treated with 2CNA-GOH or 2CNA-GPP in the presence of PMB and chloramphenicol and incubated a further 18 h. The acquired cell pellets were sonicated on ice in 500 µL lysis buffer and homogenized. PMB and chloramphenicol were added with 100 µM 2CNA-GOH or 2CNA-GPP and the samples were allowed to incubate at room temperature for 18 h. These samples were adjusted to control labeled cells via TPC and analyzed via HPLC.

2.8: Characterization of Fluorescent Products

2.8.1: Separation and Analysis of Cellular Fractions

Cells were grown and labeled for 18 h with 2CNAGOH and PMBN as mentioned above in section 2.5. Cells were pelleted as previously mentioned, however were sonicated in 500 µL 0.9% NaCl. The sample was centrifuged for 15 min at 20,000 g and the supernatant was removed; this was termed the cytosolic fraction. The remaining pellet was sonicated in 50 mM Tris pH 8, 50 mM NaCl, 0.1% Triton, and 5 mM EDTA, and homogenized; this was termed the membrane fraction. TPC was initially analyzed

for samples, however due to the extreme differences, samples were not matched. Both samples were passed through polyethylene filters. Analytical HPLC was performed on both samples using a gradient method as stated above with a mobile phase of 100 mM ammonium bicarbonate (A) and *n*-propanol (B). The cytosolic fraction was further analyzed using a method that started at 15% B and increased to 45% B over 42 min. The membrane fraction was further analyzed with a method that started at 50% B and increased to 95% B over 45 min.

2.8.2: Isolation

Isolations were conducted utilizing the aforementioned analytical c-18 HPLC column and 2CNA-GOH methods mentioned in section 2.3 with three 50 µL injections of a "well-labeled" cellular sample with 100 µM 2CNA-GOH and 15 µg/mL PMBN. All peaks present were isolated by hand based on fluorescence. Once all injections were separated, similar peaks were combined and dried under vacuum overnight. Samples were solubilized in a mix of DMSO, hexanes, chloroform, and water to remove lipid-based material from the glass, and dried again. Finally, samples were taken up in 100 µL 50% *n*-propanol and 25 mM ammonium bicarbonate for MS analysis.

2.8.3: MS

Isolated samples were suspended in a minimal amount of *n*-propanol and ammonium bicarbonate and manually injected on the Velos. Using direct infusion on a Thermo Scientific Velos Pro Electrospray ionization mass spectrometer (ESI-MS), 100 µL of samples were injected via syringe with a mobile phase of acetonitrile at 150

µL/min using a capillary temperature of 200 °C and a spray voltage of 3.6 kV. Source fragmentation was set at a potential of 45 V. Acquisitions were tested in negative ion mode.

CHAPTER THREE: DATA & RESULTS

3.1: Cellular Uptake of Isoprenoids is Possible

3.1.1: Rescue of *E. coli* from Fosmidomycin

The first goal of this project was to determine if isoprenoid uptake is possible. To reach this goal, "rescue studies" were conducted based on previous research by Oldfield.[53] The previous work has explored identifying the targets of inhibitors by unorthodox means. Compounds that were hypothesized to be suppressed were supplied exogenously; if inhibitor-treated cells were restored relative to a control, it was interpreted that the supplied compound had been suppressed (Figure 8). These studies, however, required placing bacterial cells under stress to encourage the uptake and utilization of supplemented compounds. We have adapted this approach to suit our purposes. In our rescue studies, we utilized fosmidomycin to suppress the non-mevalonate pathway with the goal of improving the incorporation of exogenous isoprenoids such as IPP or analogues or longer isoprenoid chains. The intent was not to fully rescue cells relative to a control, but verify our hypothesis that isoprenoids could not only enter cells, but also be incorporated into isoprenoid pathways.

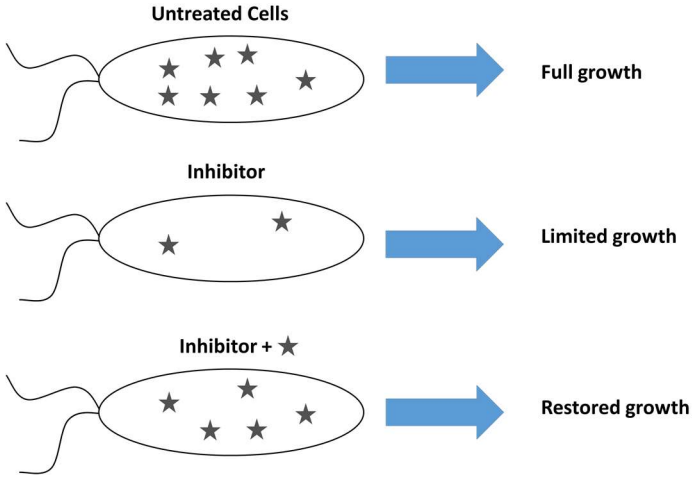

Figure 8. Conceptual depiction of rescue studies as performed by Oldfield.[22]

An MIC study was employed to find a usable concentration for fosmidomycin. For our purposes, an optimal concentration would be high enough to limit cellular growth, however would not be lethal. As IPP is vital as a building block for numerous cellular processes, we believed it unwise to completely inhibit cellular growth. For ease, we chose to measure cellular growth based on culture turbidity. Absorbance was measured by plate reader at 37 °C using clear plates. Figure 9 shows a Gompertz-fit curve that was applied to the data. Based on the calculated MIC of 13.44 μM, we chose to utilize 10 μM fosmidomycin for the remainder of our experiments.

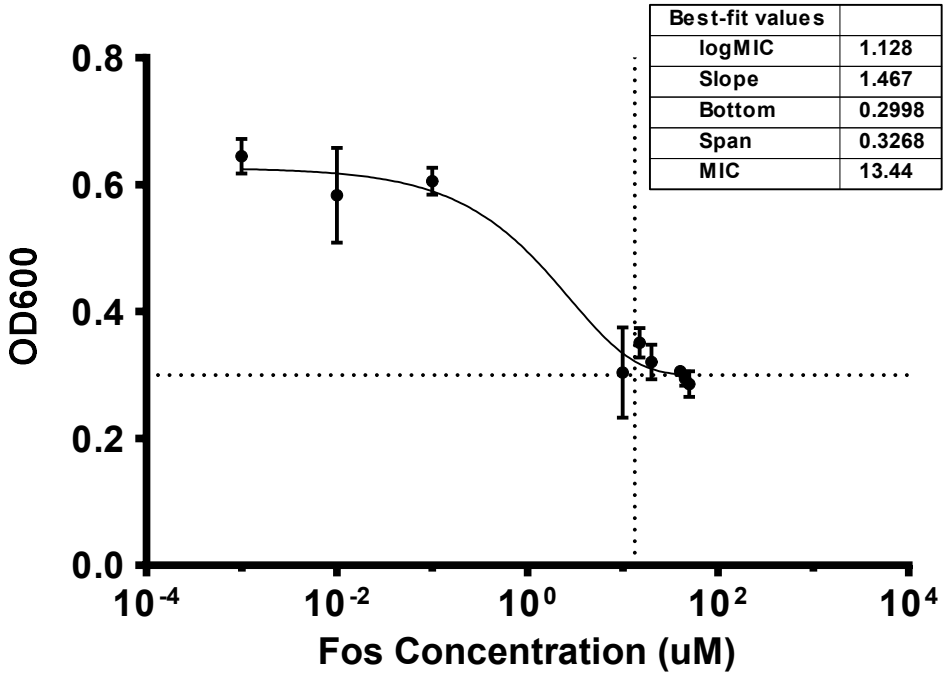

Figure 9. MIC of fosmidomycin showing the slope of the calculated curve, the lowest measured OD (bottom), and the difference between the lowest and highest measured ODs (span). The calculated MIC for fosmidomycin is 13.44 µM utilizing the *E. coli* strain MAJ427.

For the rescue studies themselves, we chose to treat cells with a gradient of IPP up to 1 mM in the presence of fosmidomycin (Figure 10). Cultures were grown for 20 h utilizing a similar method used for MIC. We chose to examine growth for up to 20 h in part based on an experiment that will be presented in section 3.2.4. In summary, this time point seemed an appropriate amount of time for fluorescent analogues to be incorporated by bacterial cells. For statistical analysis, the last 2 h of growth was averaged for each sample; this was to ensure that values were not selected which may not be representative of the overall turbidity of the samples. A student's t-test was used to compare the fosmidomycin sample to those treated with either 500 or 1000 µM IPP; comparison to the

500 μM sample resulted in a p-value of 0.04 whereas comparison to the 1000 μM sample resulted in a p-value of 0.03. We chose to use 1 mM IPP in future experiments. Though full rescue from fosmidomycin was never attained, we concluded from that IPP is capable of getting into *E. coli* cells through a currently unknown mechanism.

During these studies, we noticed that experimental cells that were treated with fosmidomycin and IPP entered the log growth phase much later relative to the control, regardless of supplemented IPP concentration. This was initially hypothesized to be due to the degradation of fosmidomycin at 37 °C, since the control culture was the only cell culture that did not show this shift in growth time. ^{1}HNMR of fosmidomycin, presented in section 3.1.2, showed that this was not the case. The next potential explanation is that the experimental cells utilized some protein to expel fosmidomycin and continue growth. This is further supported by the fact that no single culture was capable of growth at an earlier time, indicating that resistance did not spontaneously develop. Further considerations of this topic are presented in Chapter 4.

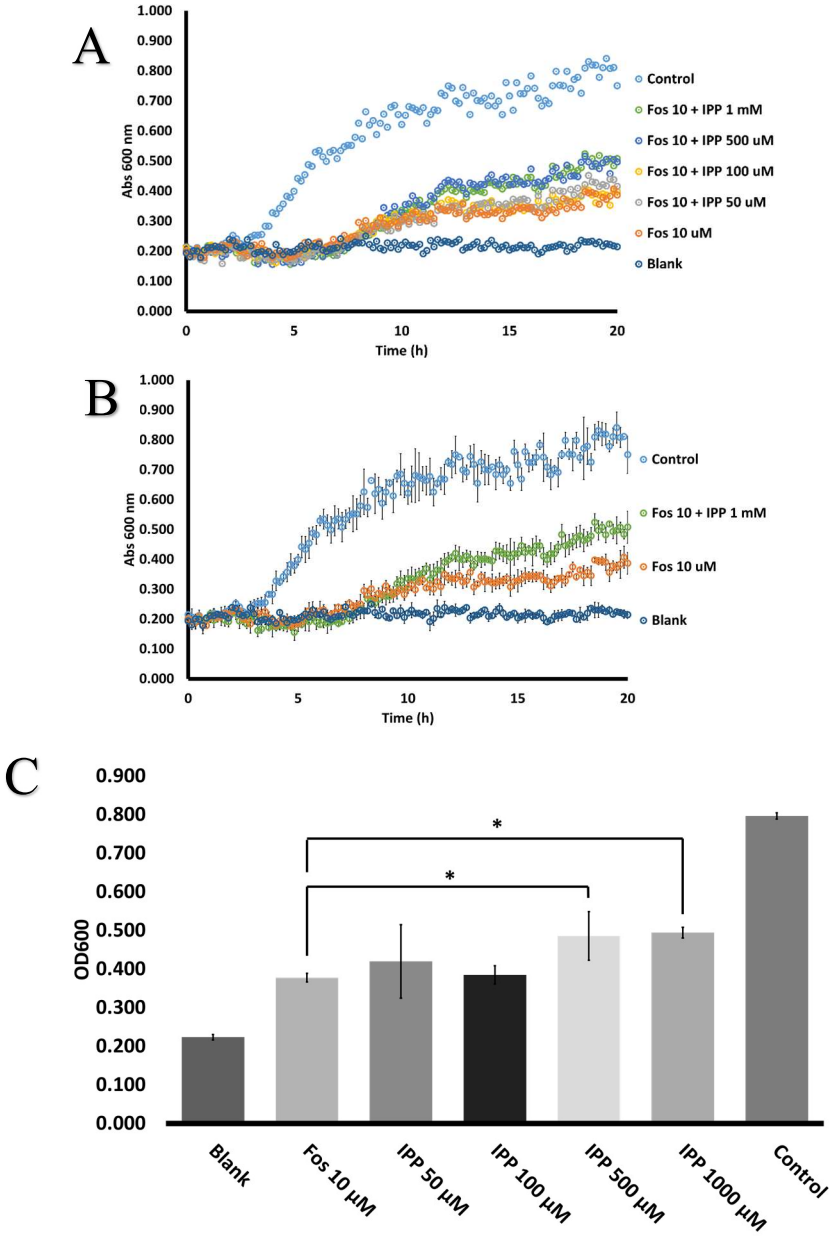

Figure 10. Triplicate rescue of *E. coli* from fosmidomycin, indicated as Fos, with varying concentrations of IPP. A) Full growth curves demonstrating growth over time as measured by absorbance. At higher concentrations of IPP, samples had greater absorbance, suggesting minimal rescue is possible. It should be noted that presented data represents complete averages, however error bars have not been included for visual clarity. B) Growth curves with selected error bars for visual clarity. C) Averages from each sample attained from the last two hours of growth including error bars. Significant differences were found between samples as indicated where one star represents $p<0.05$. It should be noted that all samples with IPP were also treated with 10 µM fosmidomycin. A student's t-test comparing the fosmidomycin sample to the 1 mM IPP sample resulted in a p-value of 0.03, indicating that these are statistically different. A t-test was also conducted comparing the fosmidomycin sample to the 500 µM IPP sample and a difference was found with a p-value of 0.04.

3.1.2: ^{1}HNMR Fosmidomycin Kinetics

Due to suspicion regarding the above rescue with IPP, we hypothesized that fosmidomycin (Figure 11) may have been degrading during incubation at 37 °C. In order to examine this potential degradation, fosmidomycin was monitored in D_2O by ^{1}HNMR at 37 °C over a period of 24 h (Figure 12). NMR was selected over other observational methods due to the ability to monitor the formation and decomposition of peaks simultaneously. Overall, no change was observed between the first and last runs. Peaks present at 1.4, 1.7, and 3.4 ppm were assigned as the three methylene units (Figure 13). The peak present at 4.6 ppm indicates the presence of H_2O. Peaks were also present at 7.8 and 8.1 ppm, and may potentially be the aldehyde, but this is uncertain as aldehydes typically arise closer to 9-10 ppm. Overall, decomposition of fosmidomycin was not observed at a temperature of 37 °C. Further considerations of this topic will be presented in Chapter 4.

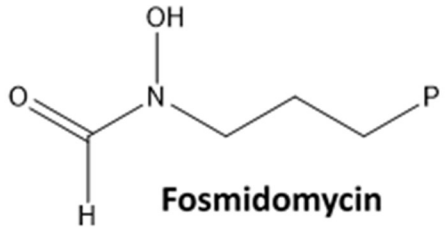

Figure 11. Structure of the antibiotic fosmidomycin. In this depiction, P represents a phosphonate group.

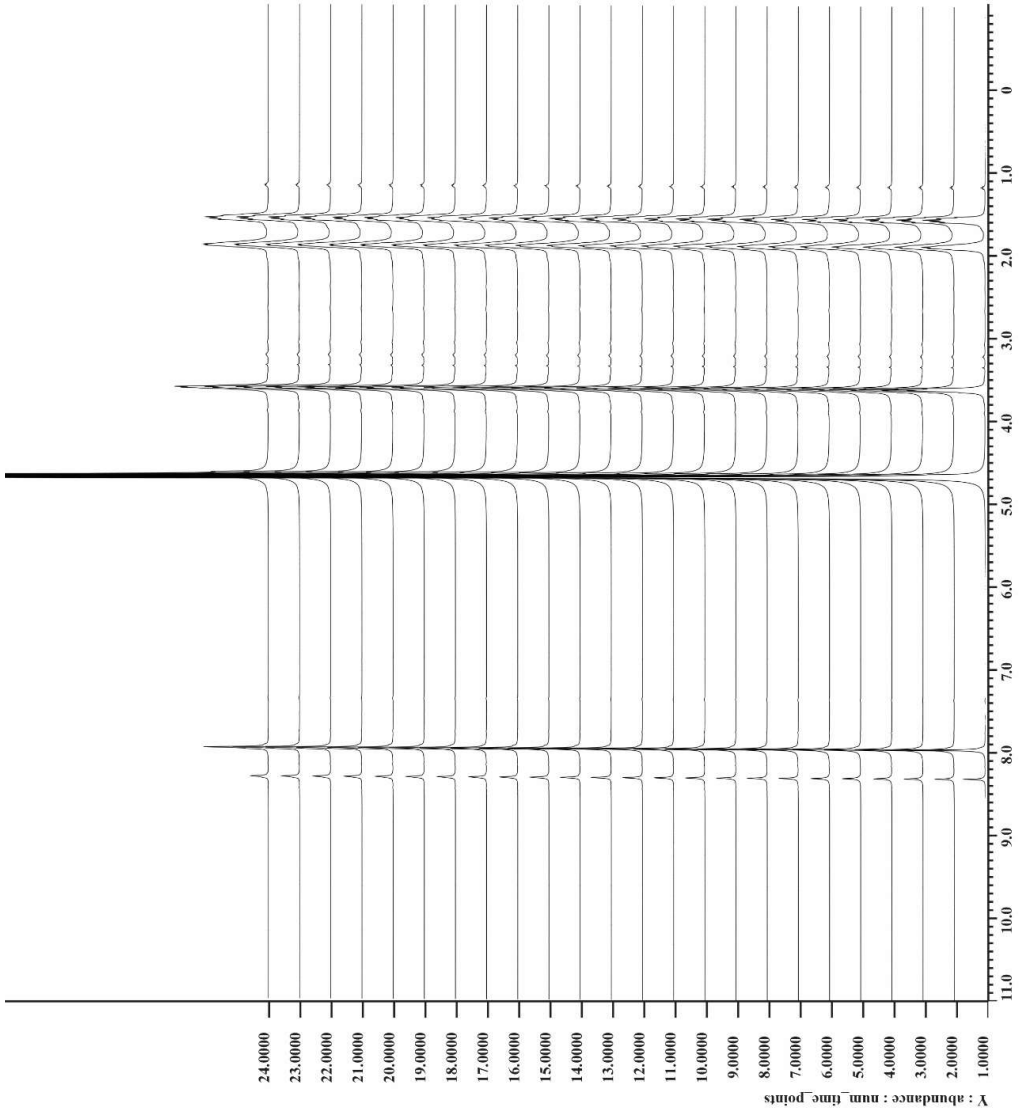

Figure 12. Kinetics of fosmidomycin in D_2O.

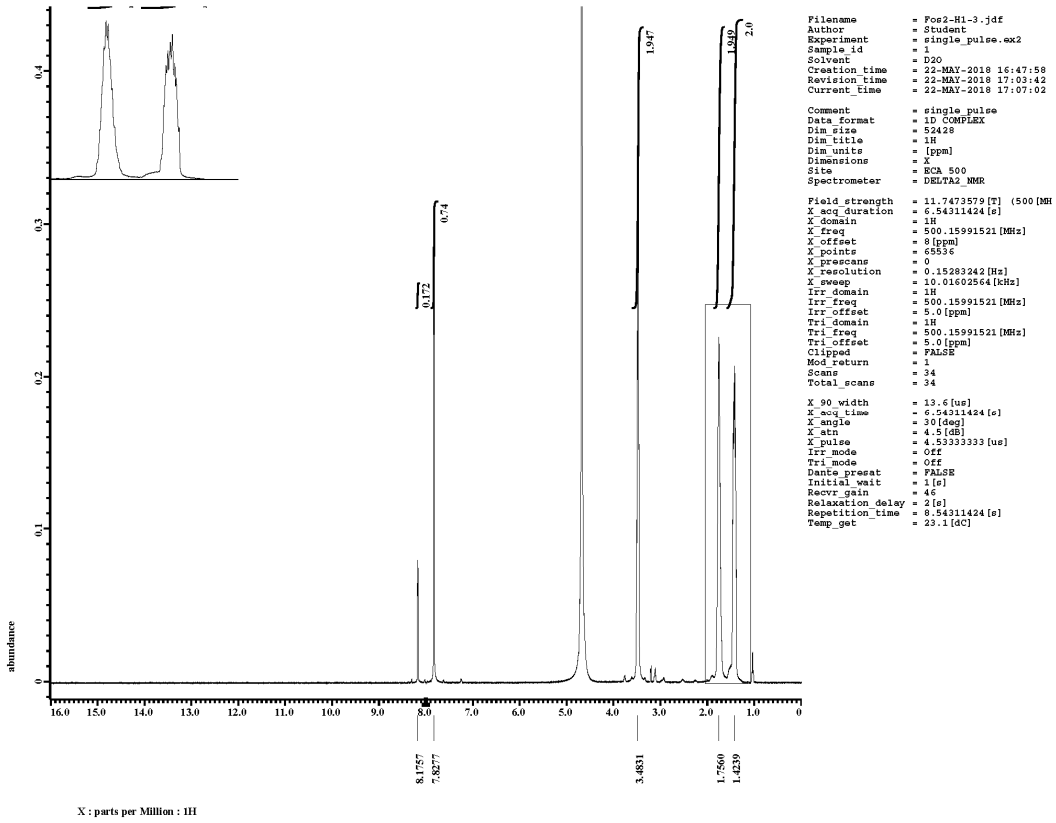

Figure 13. ^{1}HNMR of fosmidomycin in D_2O.

3.1.3: Farnesyl Diphosphate and Fluorescent Analogues Vary in Rescue Capabilities

Following the conclusion that IPP is capable of entering cell membranes, albeit to a limited degree, we chose to examine longer isoprenoids, including fluorescent FPP analogues. To this end, concentration gradients of FPP, 2CNA-GOH, and 2CNA-GPP were used in conjunction with 1 mM IPP. 2CNA-GPP was expected to be more easily incorporated into pathways than 2CNA-GOH due to the similarity to the naturally-occurring FPP, however it was also hypothesized that 2CNA-GOH would be more capable of passing through the cellular membrane due to the lack of a phosphate moiety. We anticipated that this phosphate group would impact the ability to cross the bacterial double membrane. FPP-treated cells showed

unexpected variation at different concentrations; higher concentrations seemed to have a slightly negative effect (Figure 14). The sample 5 μM FPP + 1 mM IPP was statistically different from fosmidomycin alone ($p<0.01$). However the sample with only added IPP was not statistically different from the fosmidomycin only sample ($p>0.05$). This may be due to variations in this replicate as the p-value was 0.09. Due to seemingly large error bars, a Grubb's outlier test was used for each sample; one point was removed for the 10 μM FPP + 1 mM IPP sample; no other outliers were found.

Data from cells treated with a 2CNA-GPP gradient show roughly the same amount of rescue at each concentration, suggesting that these concentrations neither help nor harm cell survival (Figure 15). Prior to quantitative analysis, a Grubb's outlier test was used on each sample; one point was removed for the 5 μM 2CNA-GPP + 1 mM IPP sample. Statistical analysis did not find any significant differences between experimental samples, other than between 10 μM Fos and 10 μM Fos + IPP + 250 μM GPP ($p<0.01$). This suggests that higher concentrations of GPP may supplement rescue past that of IPP alone. Data from 2CNA-GOH suggest that the analogue is toxic to fosmidomycin-treated cells at higher concentrations (Figure 16). In this data set, no significant differences were found.

Overall, we concluded that longer isoprenoids may be able to permeate cell membranes as seen by observed potential toxicity, however this does not appear to assist in rescue from fosmidomycin in most cases. FPP was capable of improving rescue at a low concentration and 2CNA-GPP was capable of improvement at the highest tested concentration. Either these compounds are not beneficial to cells deprived of IPP, they are not capable of permeating the cell membrane at abundant concentrations, or they cannot be easily incorporated into isoprenoid pathways. It should also be noted that this is not a perfect experimental design. Because

fosmidomycin was utilized to limit the non-mevalonate pathway and IPP production, it is not guaranteed that the addition of FPP or FPP analogues can improve rescue. It is possible that the necessary addition of IPP is sufficient for cells to form FPP, thereby not requiring the addition of further exogenously-supplied FPP. A FPP synthase inhibitor would have been more appropriate to examine FPP uptake, however one was not available for these experiments.

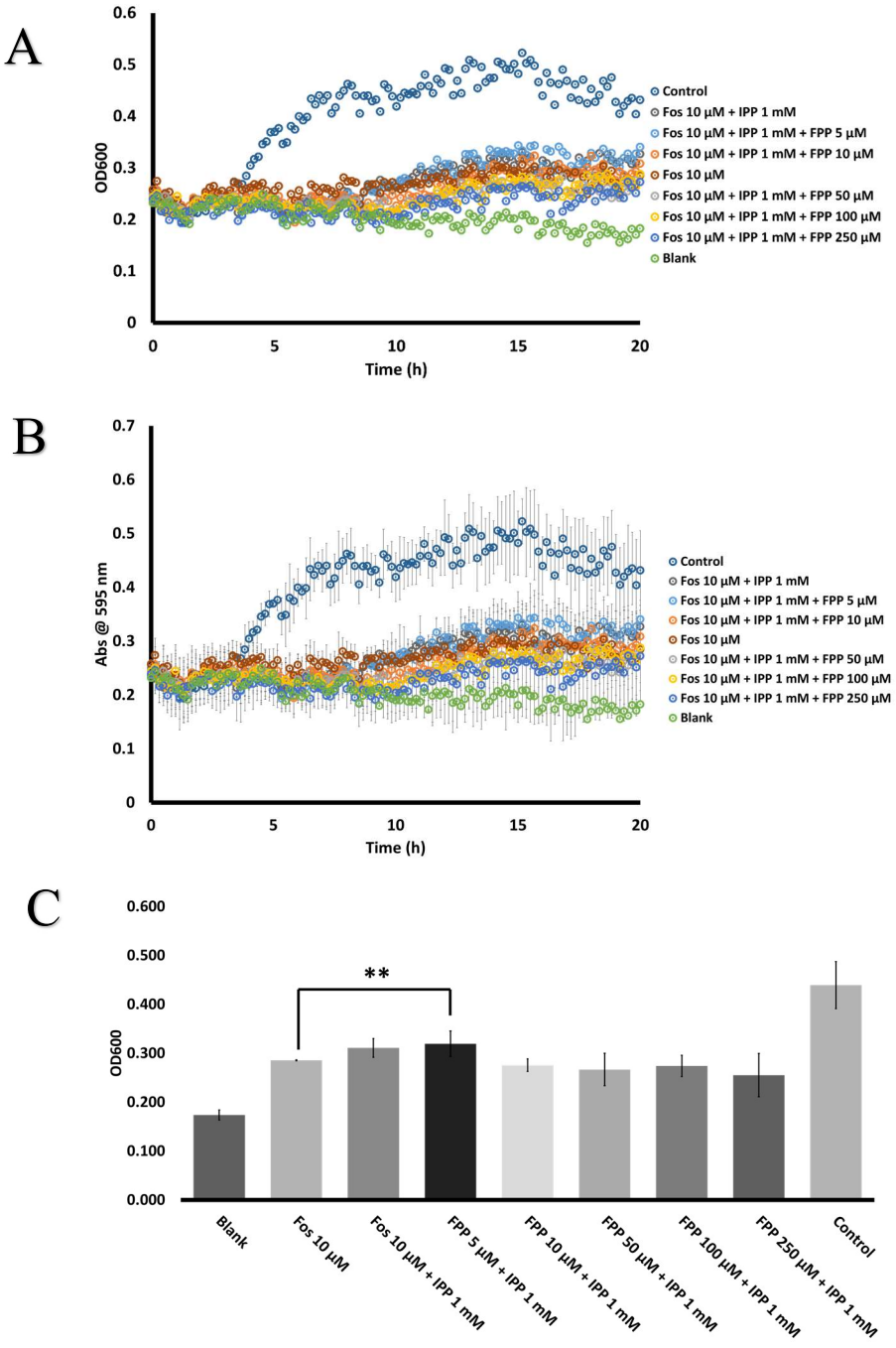

Figure 14. Triplicate rescue of *E. coli* from fosmidomycin, indicated as Fos with 1 mM IPP and varying concentrations of FPP. A) Full growth curves demonstrating growth over time as measured by absorbance. Despite increasing concentrations of FPP, experimental cultures did not match the control. It should be noted that presented data represents complete averages, however error bars have not been included for visual clarity. B) Growth curves with included error bars where n=3. C) Averages from each sample attained from the last two hours of growth including error bars. On the graph, one star represents $p<0.01$. It should be noted that all samples with FPP were also treated with 10 µM fosmidomycin. A t-test conducted between the fosmidomycin sample and the 5 µM FPP + 1 mM IPP sample resulted in a p-value <0.01.

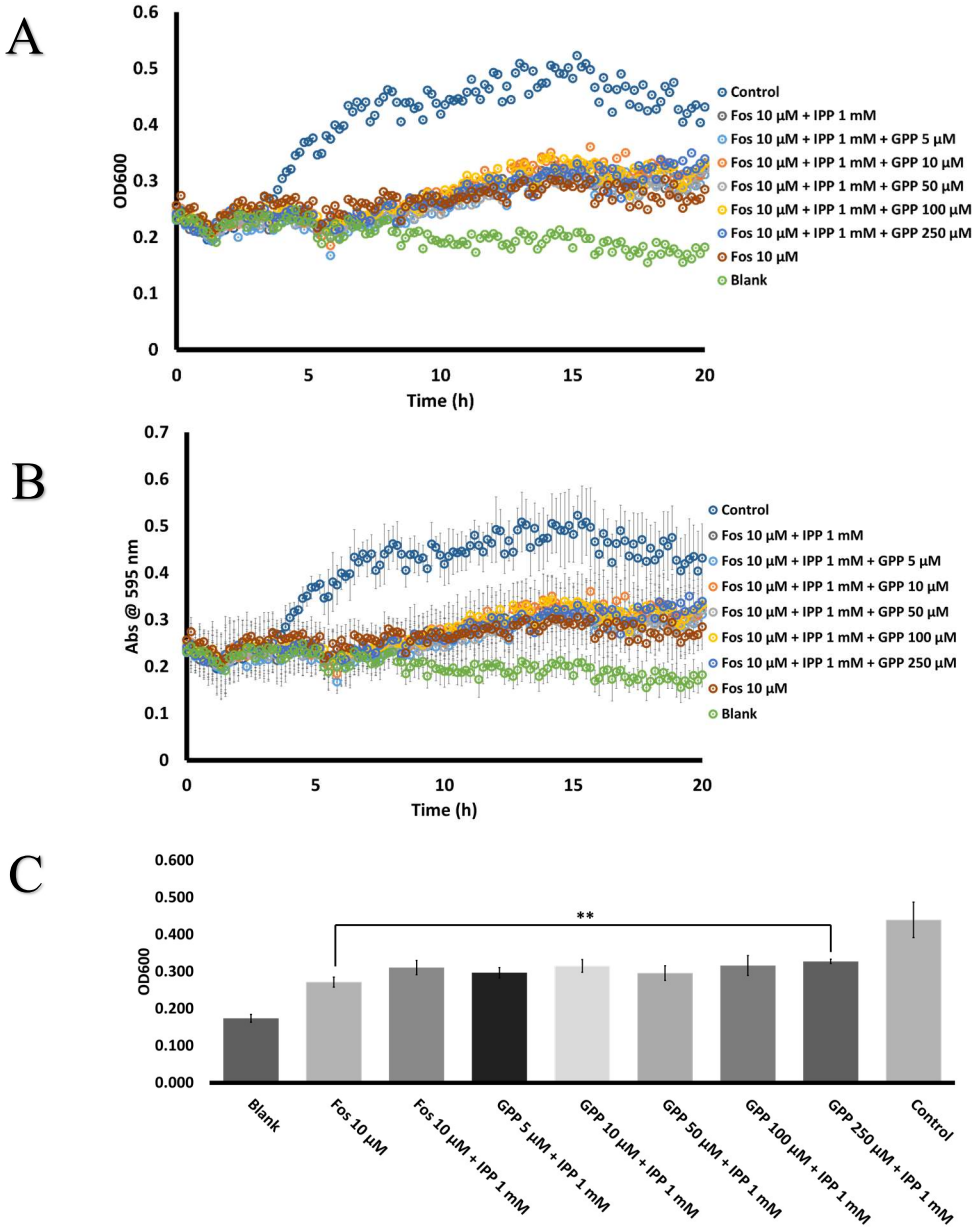

Figure 15. Triplicate rescue of *E. coli* from fosmidomycin, indicated as Fos with 1 mM IPP and varying concentrations of 2CNA-GPP, indicated as GPP. A) Full growth curves demonstrating growth over time as measured by absorbance. Even at higher concentrations of GPP, cell growth does not appear to change. It should be noted that presented data represents complete averages, however error bars have not been included for visual clarity. B) Growth curves with included error bars where n=3. C) Averages from each sample attained from the last two hours of growth including error bars. Significant differences were found between samples as indicated where two stars represents $p<0.01$. It should be noted that all samples with GPP were also treated with 10 µM fosmidomycin.

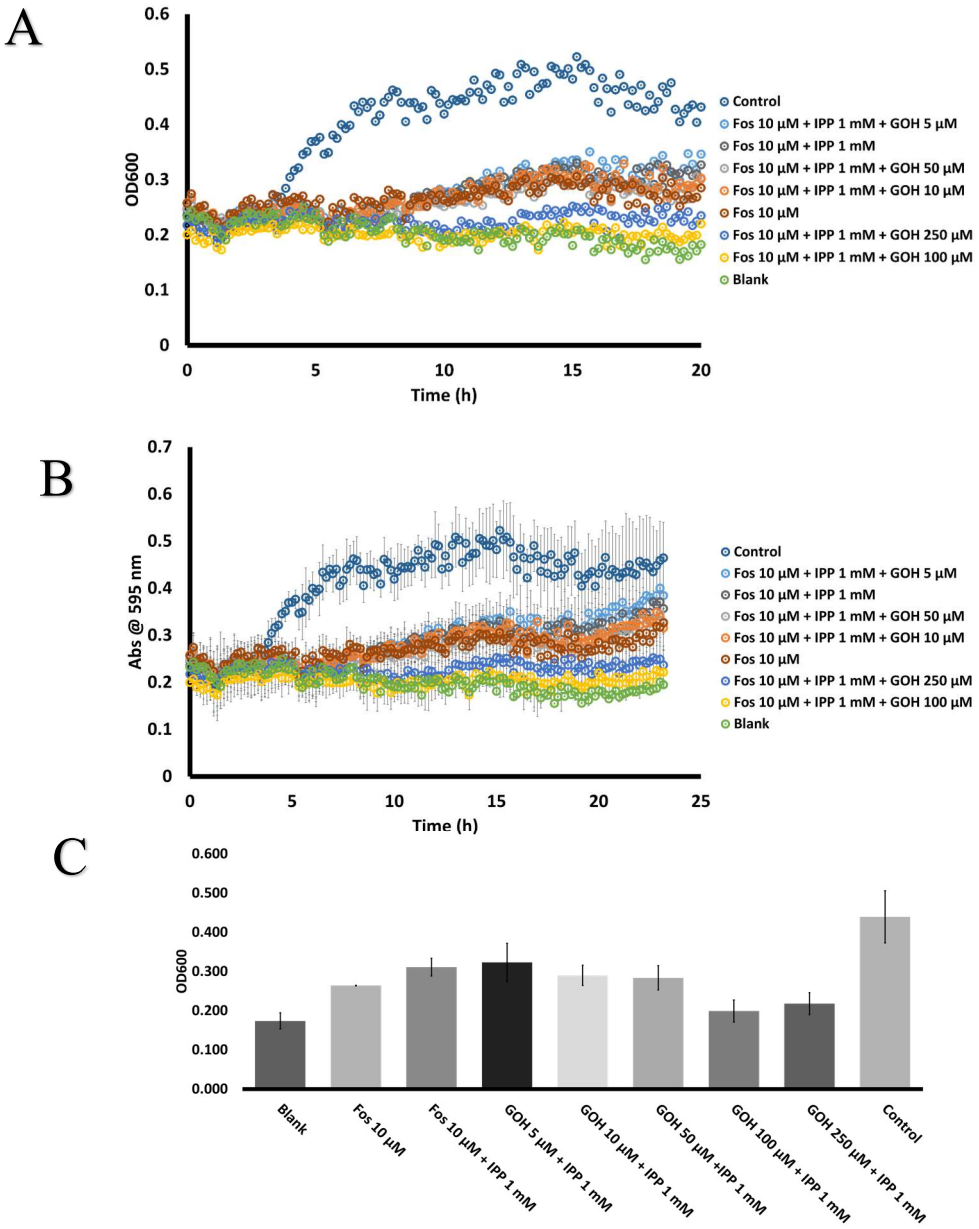

Figure 16. Triplicate rescue of *E. coli* from fosmidomycin, indicated as Fos with 1 mM IPP and varying concentrations of 2CNA-GOH, indicated as GOH. A) Full growth curves demonstrating growth over time as measured by absorbance. At higher concentrations of GOH, cell growth seemed to diminish rather than improve. B) Growth curves with included error bars where n=3. C) Averages from each sample attained from the last two hours of growth including error bars. It should be noted that all samples with GOH were also treated with 10 µM fosmidomycin. A student's t-test was conducted comparing samples and no significant differences were found.

3.1.4: Fluorescent Farnesyl Diphosphate Analogues are Toxic at High Concentrations

Following observations during rescue studies suggesting that our selected analogues may be toxic to cells at high concentrations, we next chose to establish an upper limit of analogue that cells could tolerate; these experiments were termed toxicity studies. Similarly to MIC and rescue studies, these experiments were conducted in 96-well plates at 37 °C and data points were measured via absorbance. We hypothesized that cells could tolerate only a limited amount of analogue and therefore anticipated identifying a concentration that impacted survivability. Further, we did not expect them to be able to export or metabolize the analogues to the point of compensation at high, potentially lethal concentrations. For this set of experiments, we chose to examine concentrations of 2CNA-GOH up to 1 mM and 2CNA-GPP up to 750 μM.

The measured absorbances of cells grown in the presence of either fluorescent analogue matched closely with those of the controls (Figure 17). Even at high concentrations, neither 2CNA-GOH nor 2CNA-GPP appeared to have an impact on cell growth. Based on this observation in combination with those made during rescue studies, we hypothesized that assistance is likely required for these compounds to permeate the bacterial cell membrane. We chose to examine EDTA, PMB, and PMBN for improved membrane permeability; these will be discussed in detail in a further section. We ultimately chose to implement PMBN in conjunction with our fluorescent analogues in experiments.

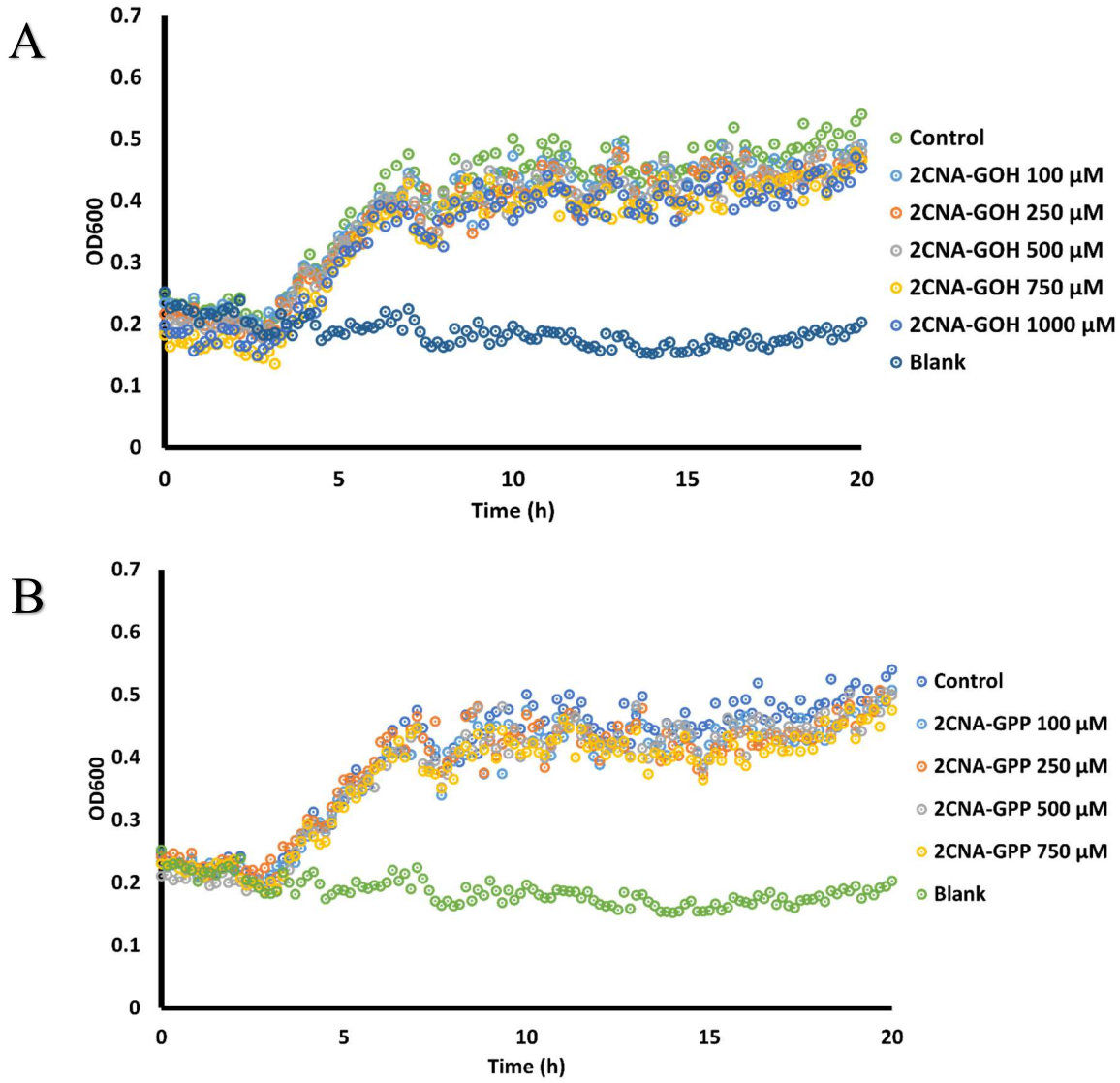

Figure 17. Toxicity of A) 2CNA-GOH and B) 2CNA-GPP at 37 °C over 20 h as measured by absorbance. Concentrations of up to 1 mM for 2CNA-GOH and 750 µM for 2CNA-GPP did not appear to impact cell turbidity compared to a control culture. It should be noted that the presented data is the average of a performed triplicate; error bars are not presented for visual clarity.

When PMBN was added at 15 µg/mL in conjunction with analogues, maximum cell growth steadily declined with increasing analogue concentration (Figure 18). This was especially prominent with 2CNA-GOH compared to 2CNA-GPP; the cultures containing 750 and 1000 µM 2CNA-GOH showed the least overall growth, whereas similar concentrations of 2CNA-GPP appeared to have less of an impact. This suggests that these analogues not only are

toxic to bacterial cells at high concentrations, but also that the compounds must first be able to pass through the cell membrane for any significant impact to be observed.

Statistical comparison of cultures treated with or without PMBN was conducted similarly to rescue studies; the last 2 h of growth was averaged for each sample in each replicate to ensure that values were not selected which may not be representative of the overall turbidity of the samples (Figure 19). Prior to all analysis, a Grubb's outlier test was conducted and outliers were removed. For 2CNA-GOH, statistical differences were not found between samples treated with or without PMBN based on conducted t-tests. For 2CNA-GPP, statistical differences were found between samples treated with or without PMBN at 100 ($p<0.05$) and 500 μM ($p<0.05$) concentrations. There was also a significant difference between the PMBN control and the 2CNA-GPP 500 μM sample ($p<0.05$).

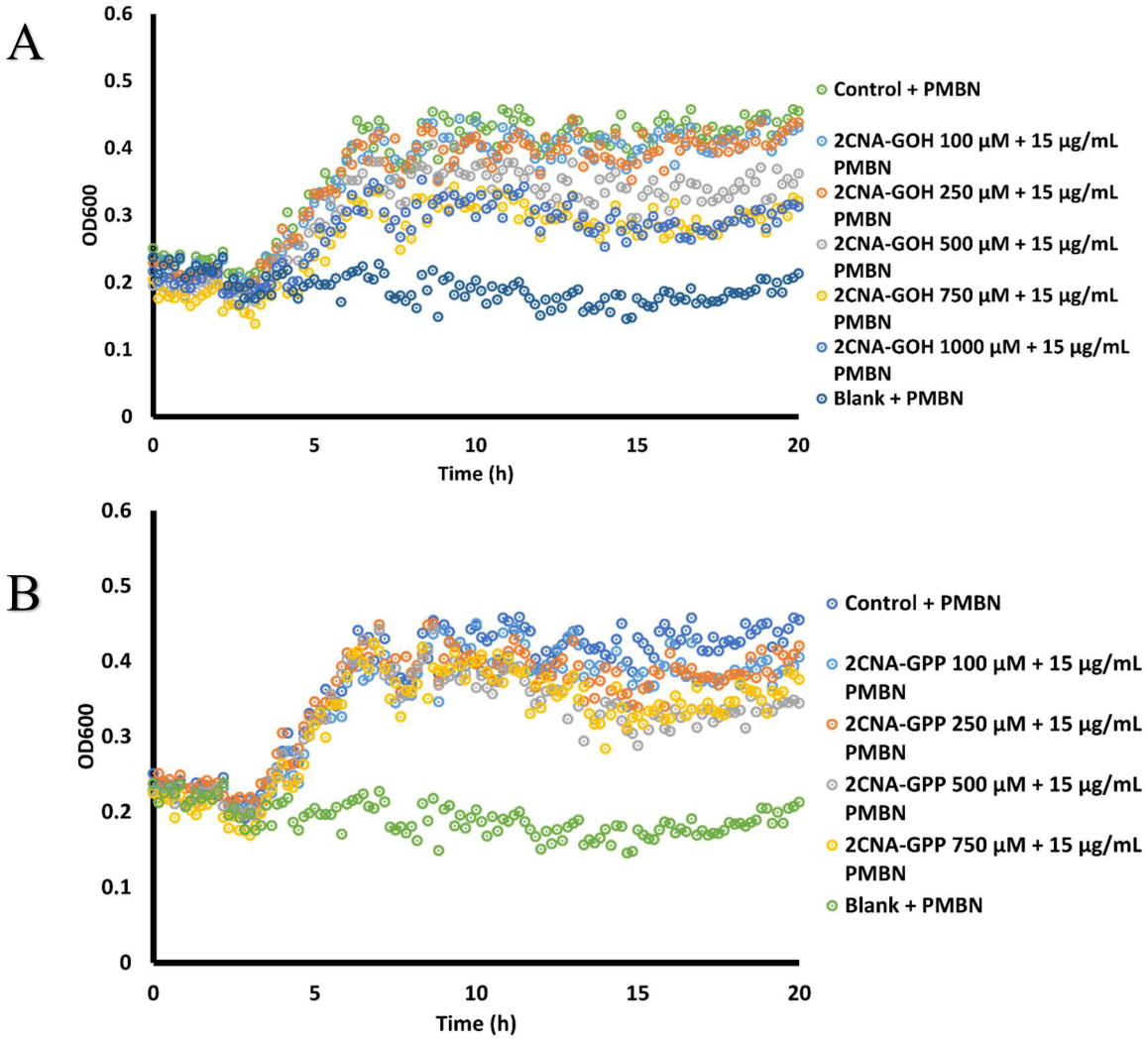

Figure 18. Toxicity of A) 2CNA-GOH and B) 2CNA-GPP with 15 µg/mL PMBN at 37 °C over 20 h. High concentrations of 2CNA-GOH impacted cell turbidity suggesting toxicity when the compound was capable of permeating the cell membrane. While high concentrations of 2CNA-GPP did not appear to have as strong of an impact as 2CNA-GOH, differences were still observed with increasing concentration. Note that presented data is an average of three replicates; error bars have not been included for visual clarity.

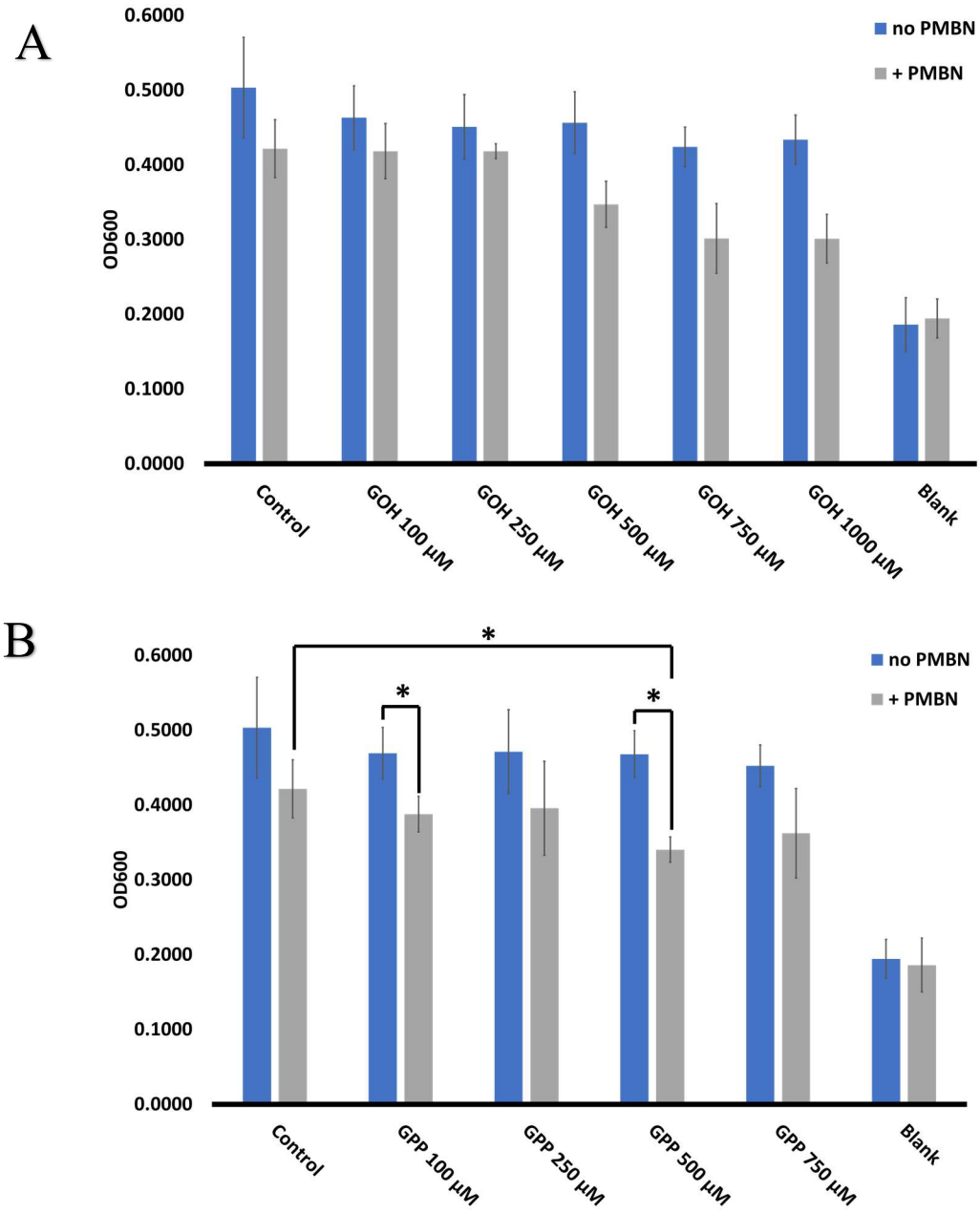

Figure 19. Comparison of final OD measurements from examined A) 2CNA-GOH, indicated as GOH, and B) 2CNA-GPP, indicated as GPP, cultures with and without PMBN. Final measurements are averages from the last 2 h of growth for each sample to ensure that values were not selected which may not be representative of the overall turbidity of the samples. Statistical analysis was performed in the form of t-tests for each concentration and for each sample n=3. Significant differences were found between samples as indicated where one star represents $p<0.05$.

3.2: Cellular Incorporation of 2CNA-GOH and 2CNA-GPP

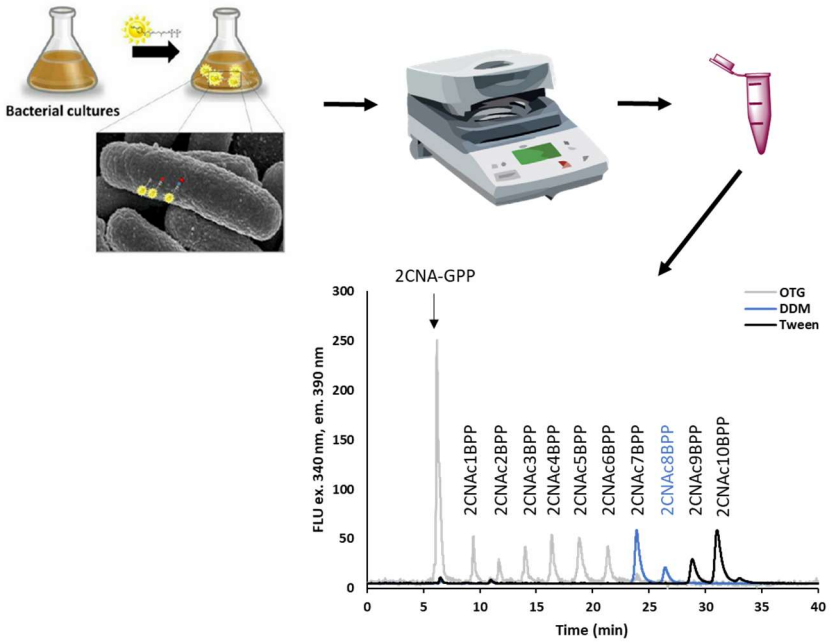

Figure 20. Conceptual methodology for cellular labeling. Cells are first labeled with analogue, presumably being incorporated into isoprenoid pathways. Following growth, cells are pelleted, washed, lysed, and prepared for analysis via HPLC. It is anticipated that BPP products similar to those observed during controlled UppS reactions will form. In the chromatogram from standards, the naturally occurring BPP length is indicated in blue text. Figure adapted from Troutman.

Thus far, toxicity studies incorporating PMBN have suggested that FPP analogues are capable of passing through bacterial cell membranes, however rescue studies suggest the opposite. The fluorescent moiety on these compounds, however, allows us to examine whether or not these compounds are utilized by cells by HPLC analysis. Fluorescent analogues were added to cells prior to growth to examine uptake and incorporation into isoprenoid pathways following our general methodology (Figure 20). We expected the formation of hydrophobic (retention time $\geq$ 20 min) products such as BP and BPP, assuming the analogues were capable of permeating the cellular membrane. We observed during toxicity and rescue studies that exceedingly high concentrations of 2CNA-GOH could result in limited cellular growth, so we chose to limit analogue concentrations to 100 μM; this limit was also applied to 2CNA-GPP for comparison. Compared to untreated controls, cells grown in the presence of 2CNA-GOH or 2CNA-GPP show

fluorescent peaks at an excitation and emission of 340 and 390 nm in both hydrophobic and hydrophilic (retention time ≤ 20 min) regions (Figure 21). We expect retention times of approximately 7 and 13.5 min for 2CNA-GPP and 2CNA-GOH, respectively, based on standards. Depending on the number of added isoprene units, BPP products may occur between 9 and 33 min, based on standards and shown in Figure 20. Comparison to the LB supernatant and standards shows that products in the cellular material are unique to that material. This suggests that these compounds are not only getting through the cell membrane, but also that they are either being incorporated into appropriate pathways or metabolized in such a way that maintains the fluorescent properties of the nitrileaniline moiety. Products present in the LB are limited to hydrophilic regions. These may represent degraded versions of the analogues, such as a monophosphate in the case of 2CNA-GPP, or products that were released from bacteria.

It should be noted that 2CNA-GOH shows similar labeling compared to 2CNA-GPP, even with similarly adjusted total protein concentrations, which is intended to normalize the amount of cellular material analyzed for appropriate comparison. We had previously hypothesized that the alcohol would be better able to permeate the cellular membrane compared to the diphosphate due to the charged nature of the diphosphate; without an active uptake mechanism, an alcohol should more easily diffuse across the cell membrane. However, the data suggest that both analogues can be incorporated by cells to a similar degree.

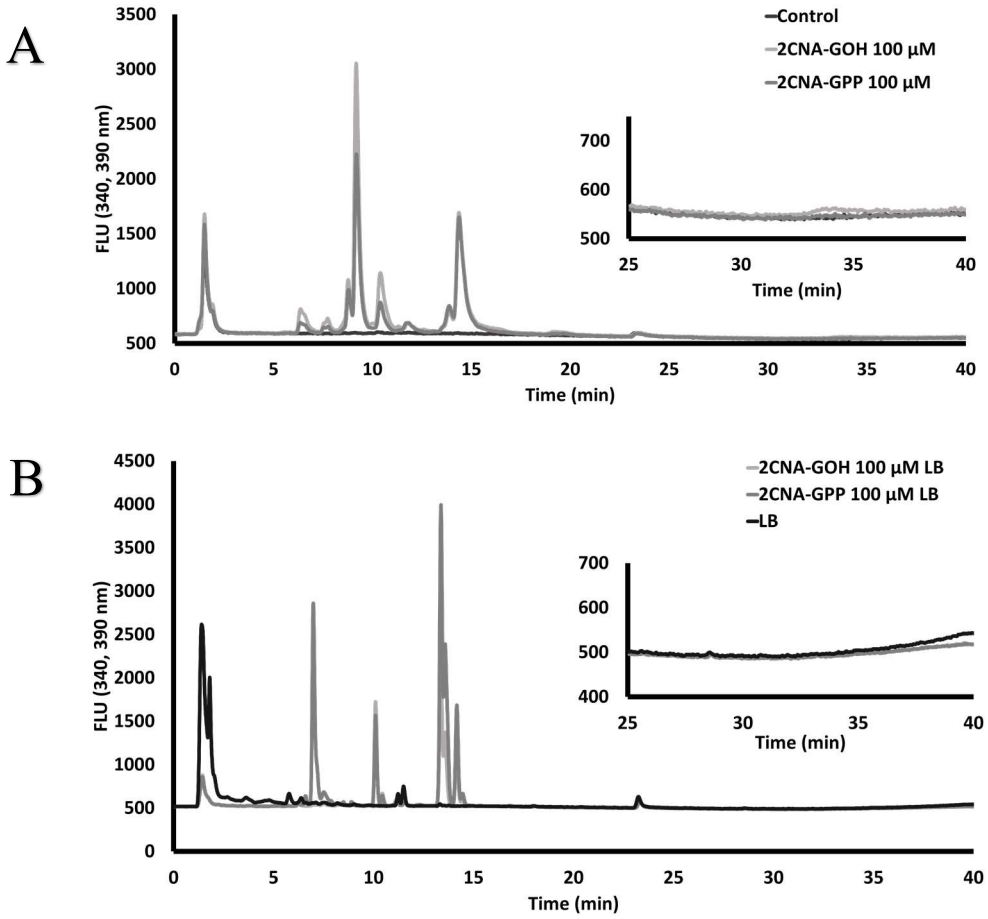

Figure 21. A) Comparisons of cellular incorporation of 2CNA-GOH and 2CNA-GPP. Total protein content was adjusted to 1 mg/mL and 20 µL were injected for HPLC analysis. Both the alcohol and diphosphate analogues appear to be incorporated into pathways to a similar degree as observed by relative peak height and peak abundance. B) Comparisons of LB from the cellular incorporation of 2CNA-GOH and 2CNA-GPP. Peaks other than those from the analogues themselves are present, suggesting that either modified materials have been released into the growth media, or that modifications are occurring to the analogues in the growth media itself.

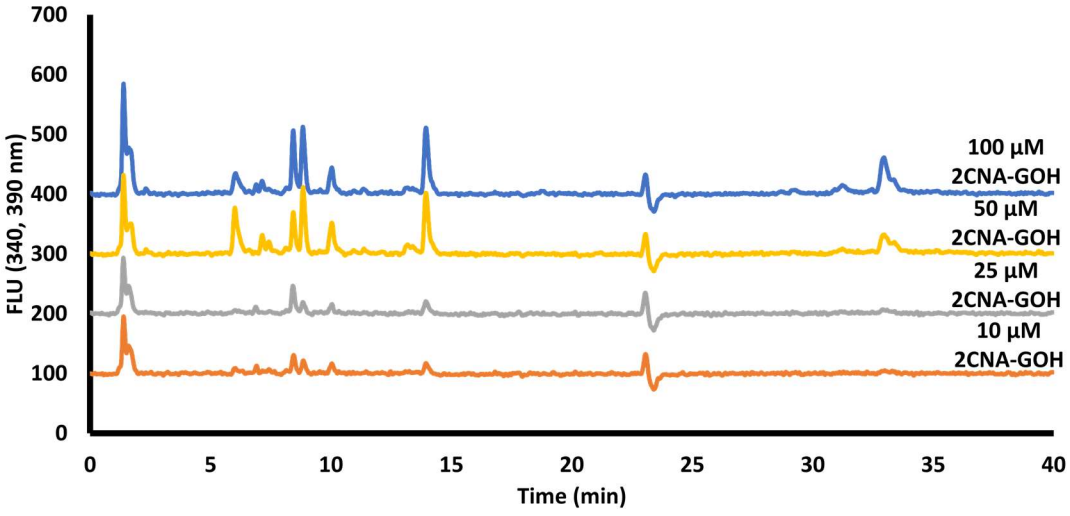

Figure 22. Comparisons of various concentrations of 2CNA-GOH. Higher concentrations of the alcohol correlated with the appearance and larger size of hydrophobic peaks between 30 and 35 min.

Table 2. Percent relative increases of samples treated with varying concentrations of 2CNA-GOH relative to either 10 or 25 µM 2CNA-GOH samples at selected retention times. The selected retention times are predicted to be the 2CNA-GOH peak (13.9 min) and BP or BPP products (33 min). Product formation of the 33 min peak was not observed in the 10 µM 2CNA-GOH sample and therefore the next concentration was used for comparative analysis.

2CNA-GOH Concentration (µM)	Integrated area at 13.9 min	% of Total Area (%)	% Increase Relative to 10 µM (%)	Integrated area at 33 min	% of Total Area (%)	% Increase Relative to 25 µM (%)
10	851.9	16.54	-	-	-	-
25	863.5	15.41	1.34	120.9	2.16	-
50	2453.9	18.16	65.28	411.1	3.04	70.59
100	2617.6	18.06	67.45	1410.9	9.74	91.43

To ensure that the selected concentration of 100 µM 2CNA-GOH was optimal, various concentrations of the analogue were tested. Specifically, we chose to examine lower concentrations to determine if an analogue concentration of 100 µM was required to observe labeling. As shown in Figure 22, similar amounts of labeled products are seen in the hydrophilic region at 50 and 100 µM, however, there is much less hydrophobic product formation at 50 µM. Relative to the 25 µM where hydrophobic products are first observed, the 50 µM 2CNA-GOH sample has an integrated area more than 20% smaller than that of the 100 µM 2CNA-GOH sample (Table 2). Lower concentrations resulted in even fewer fluorescent products and were therefore not considered for further use. We have interpreted this to suggest that the concentration of 100 µM for 2CNA-GOH may result in better labeling of these products.

3.2.2: EDTA and PMB Impacts on Membrane Permeability

Initial experiments presented in section 3.2 that utilized 2CNA-GOH and 2CNA-GPP showed lower levels of cellular labeling than expected. Likewise, observations made during toxicity studies suggested that our selected analogues were not capable of successfully permeating the cell membrane. We therefore explored the option of using a membrane

permeabilization compound to assist with analogue uptake. EDTA and PMB were both tested for their respective impacts on membrane permeability. We selected EDTA due to its chelating nature; compounds such as this are believed to disrupt the membrane by disrupting Mg^{2+} and Ca^{2+} ions in the membrane, increasing passive diffusion .[28, 40] PMB was selected due to its ability to interact with the LPS portion of the cellular membrane. The fatty acid portion of this antibiotic is believed to intercalate in such a way that the outer membrane is disrupted and ultimately compromises membrane stability.[41]

Prior to incorporation in labeling protocols, MICs were conducted on both of these compounds (Figure 23). It should be noted that while these studies are MICs, our intent was not to find a concentration that would be lethal to cells. Instead, we wanted to find a concentration that clearly impacts cells while not fully inhibiting growth. This is defined as the non-inhibitory concentration (NIC), the highest concentration before cellular impacts are observed. Based on the literature, we explored ranges around 0.5 μg/mL for PMB.[54] EDTA is typically used to fully inhibit growth, however has been used to assist the uptake of other compounds; we chose to mainly focus on concentrations between 1 and 10 mM.[55]

Based on estimated NICs from the MIC curves, we chose to further examine 1 mM EDTA and 0.01 μg/mL PMB, as well as concentrations one magnitude above and below for HPLC analysis; these were examined in conjunction with 100 μM 2CNA-GOH. For EDTA, 0.1, 1, and 10 mM were tested (Figure 24) while for PMB, 0.001, 0.01, and 0.1 μg/mL were tested (Figure 25). Total protein content for each sample was adjusted to 0.5 mg/mL prior to HPLC analysis. Overall, minimal labeling is seen in the presence of both compounds. It should be noted that the initial number of cells is not comparable to that in the MICs, therefore the concentrations selected were not lethal, even if suggested as such by the MIC. However, cell

samples treated with 10 mM EDTA showed significantly less growth with visually smaller pellets post-centrifugation (pellet size not shown). Further, due to this limitation, the total protein concentration for the 10 mM EDTA sample was roughly half of all other samples following a Bradford Assay and adjustment (0.25 mg/mL). In the 0.1 mM EDTA sample, small peaks are visible in the hydrophobic region between 30 and 35 min.

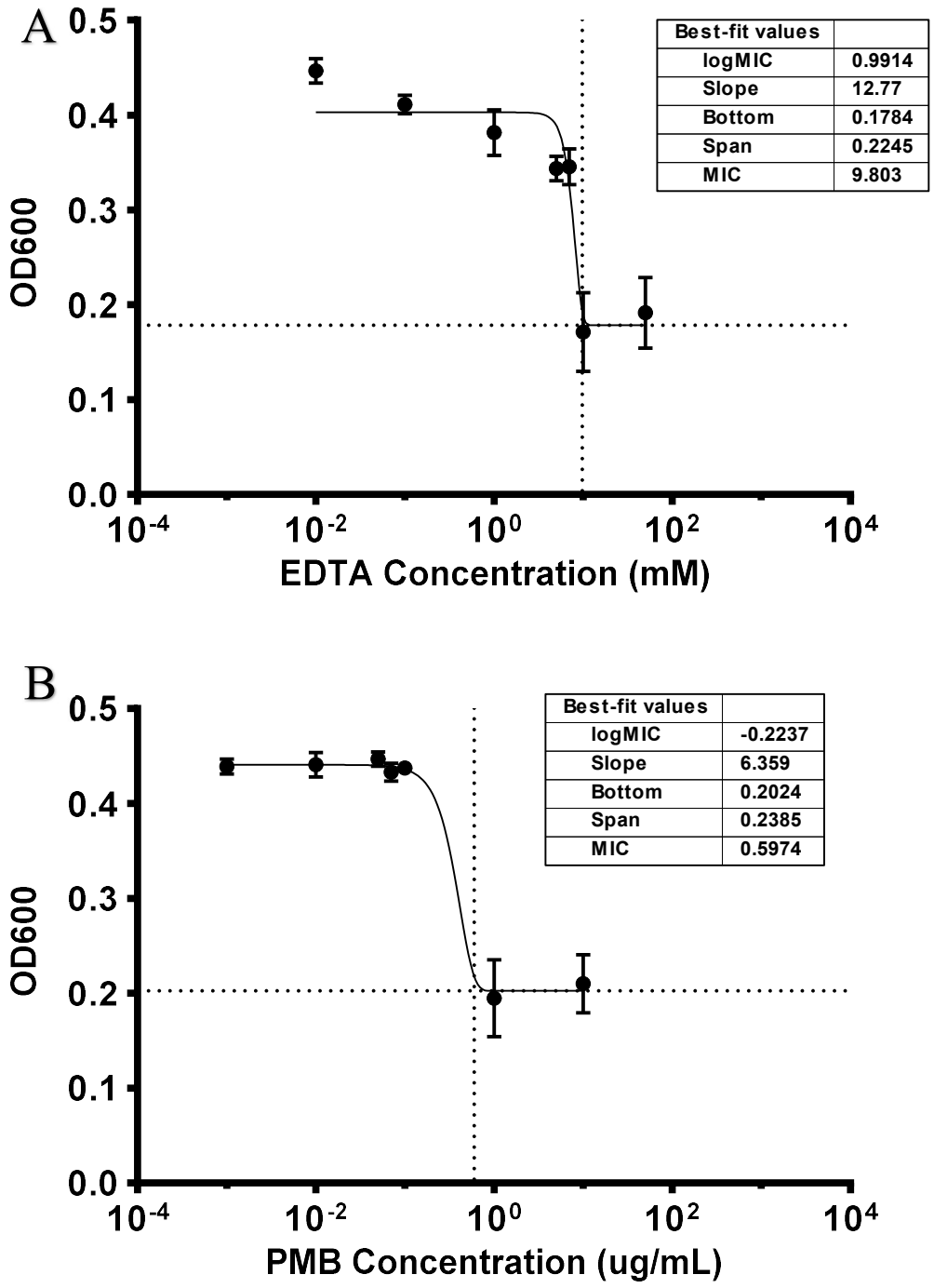

Figure 23. MIC curves of A) EDTA and B) PMB on *E. coli* strain MAJ427. In both figures, the slope of the calculated curve, the lowest measured OD (bottom), and the difference between the lowest and highest measured ODs (span) are displayed. The calculated MIC for EDTA is roughly 10 mM and the MIC for PMB is roughly 0.6 µg/mL utilizing this *E. coli* strain.

Tables 3 and 4 present integrated areas of selected retention times. Based on these values, we have concluded that 1 mM EDTA and 0.01 μg/mL PMB are the best concentrations for labeling in these sets. However, this does not necessarily mean that these are optimal or demonstrate successful labeling. Based on controlled enzyme reactions with UppS, we anticipated peaks to appear at later retention times indicative of fluorescently-labeled BP or BPP formation (Figure 20). Since these peaks are not present, we chose to examine another membrane permeabilizer, PMBN.

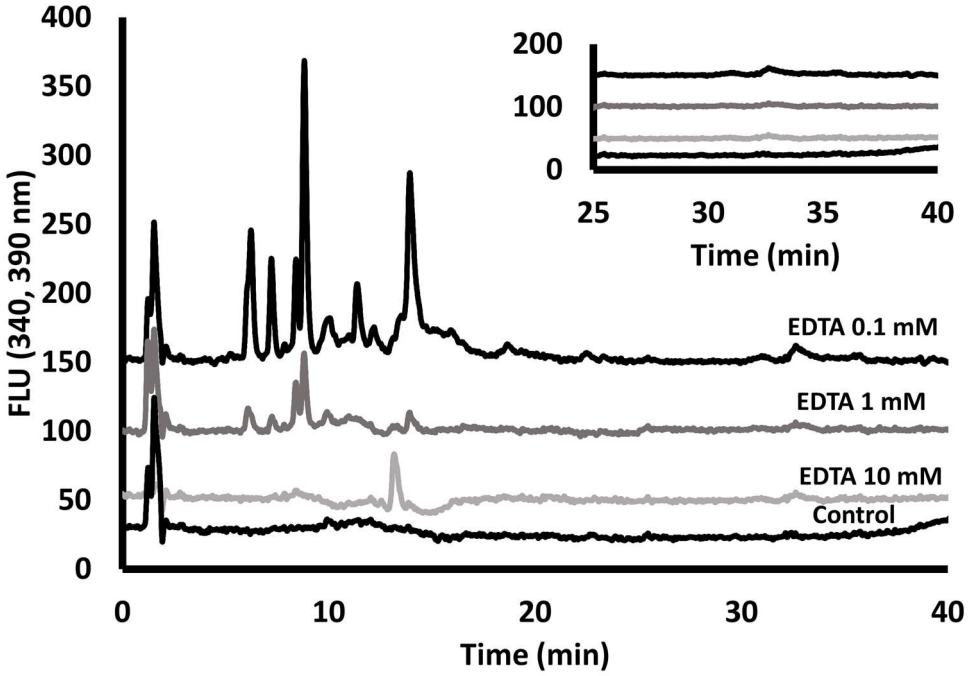

Figure 24. HPLC comparison of cells treated with different concentrations of EDTA. Total protein content was adjusted to 0.5 mg/mL for each sample when possible. It should be noted that the total protein content for the highest concentration of EDTA is roughly half of the others due to limited cell pellet size. An inset is provided for better visualization of later peaks.

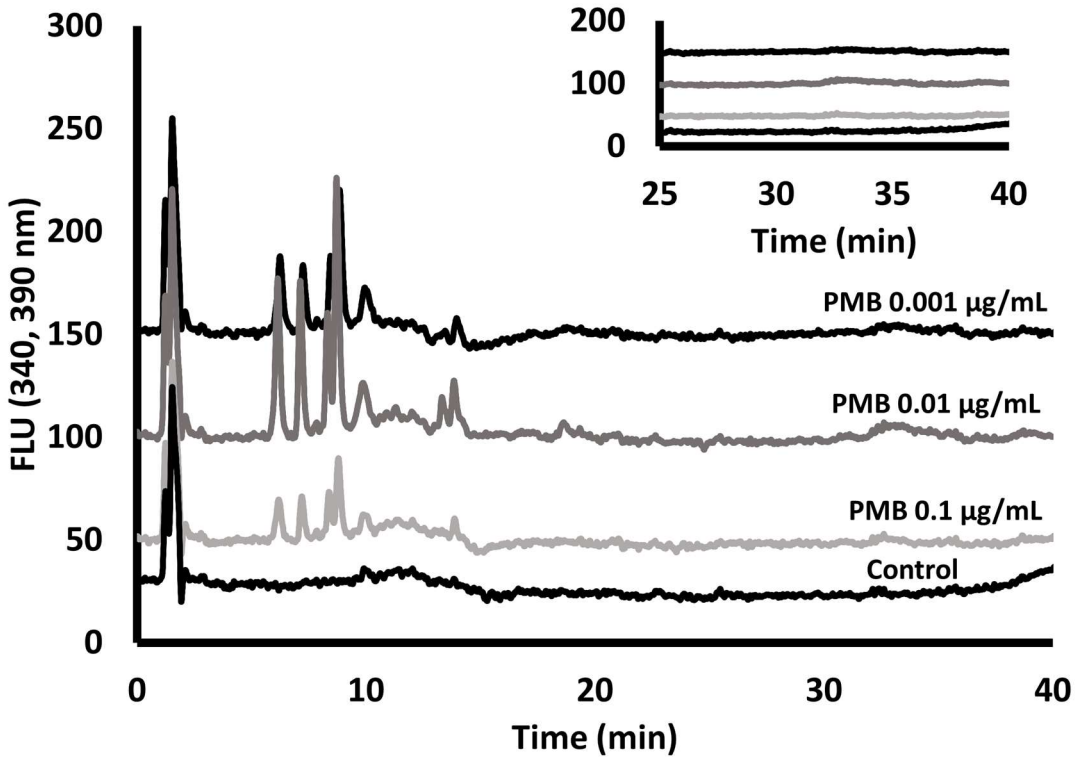

Figure 25. HPLC comparison of cells treated with different concentrations of PMB. All total protein content values match relative to the control and were adjusted to 0.5 mg/mL for each sample. No peaks are present in the hydrophobic region, suggesting that fluorescent-labeled BP was not formed in excess. An inset is provided for better visualization of later peaks.

Table 3. Percent relative increases of samples treated with varying concentrations of PMB relative to a sample treated with 0.1 µg/mL PMB at selected retention times. The selected retention times are among the most prominent and are intended to be representative of overall product formation. The 13.9 min retention time was selected because this is commonly the retention time for 2CNA-GOH.

PMB Concentration (ug/mL)	Integrated area at 6.2 min	% of Total Area (%)	% Increase Relative to PMB 0.1 µg/mL	Integrated area at 8.8 min	% of Total Area (%)	% Increase Relative to PMB 0.1 µg/mL	Integrated area at 13.9 min	% of Total Area (%)	% Increase Relative to PMB 0.1 µg/mL
0.001	759.4	22.52	48.72	934.8	27.72	41.20	191.5	5.681	46.37
0.01	1242.6	19.46	68.66	1747.7	27.38	68.55	424.6	6.65	75.81
0.1	389.4	19.10	-	549.7	26.96	-	102.7	5.035	-

Table 4. Percent relative increases of samples treated with varying concentrations of EDTA relative to a sample treated with 1 mM EDTA at selected retention times. 10 mM EDTA is not presented due to general lack of peaks. The selected retention times are among the most prominent and are intended to be representative of overall product formation. The 13.9 min retention time was selected because this is commonly the retention time for 2CNA-GOH.

EDTA Concentration (mM)	Integrated area at 6.2 min	% of Total Area (%)	% Increase Relative to EDTA 1 mM	Integrated area at 8.8 min	% of Total Area (%)	% Increase Relative to EDTA 10 mM	Integrated area at 13.9 min	% of Total Area (%)	% Increase Relative to EDTA 1 mM
0.1	1827	9.97	80.95	3053.1	16.652	75.14	5697	31.072	78.62
1	348.1	5.01	-	758.9	10.927	-	1218.1	17.54	-
10	-	-	-	-	-	-	-	-	-

3.2.3: PMBN Assists with Membrane Permeation

Following cellular labeling with EDTA and PMB, we chose to test the efficacy of PMBN, a modified form of PMB that displays decreased lethality while maintaining membrane permeability functionality.[56] Similarly to EDTA and PMB, we chose to conduct an MIC prior to cell labeling (Figure 26). However, this experiment was conducted to demonstrate that *E. coli* cells are not susceptible to any potentially lethal effects for PMBN concentrations used in our experiments. Prior research has shown that the *E. coli* strain ATCC 25922 was susceptible to PMBN at a concentration of 32 μg/mL, however it should be noted that this particular strain was intended for antibiotic susceptibility.[54] We therefore anticipated that a concentration of less than 30 μg/mL would yield desired results without potentially interfering with cell survival. Because the MIC study in this case is intended to demonstrate that PMBN is not lethal, we did not test concentrations that were meant to fully kill cells. Thus, the Gompertz-fit MIC curve for PMBN is not presented due to the inability of the compound to kill cells even at a concentration of 50 μg/mL.

We treated cell cultures with a concentration gradients of PMBN, and settled on an ideal concentration between 15 and 30 μg/mL. For these studies, we maintained control cultures, as well as cultures without any PMBN for comparison, and expected better cellular labeling in the presence of PMBN, based on maximum fluorescence. Cells treated with only analogues show less overall labeling than those treated with analogues in the presence of 15 μg/mL PMBN (Figure 27). This is especially true for cultures treated with 2CNA-GPP, possibly due to the charged nature of the diphosphate. In the

presence of PMBN, GPP cultures had increased number of total peaks as well as fluorescence, even when total protein content was matched.

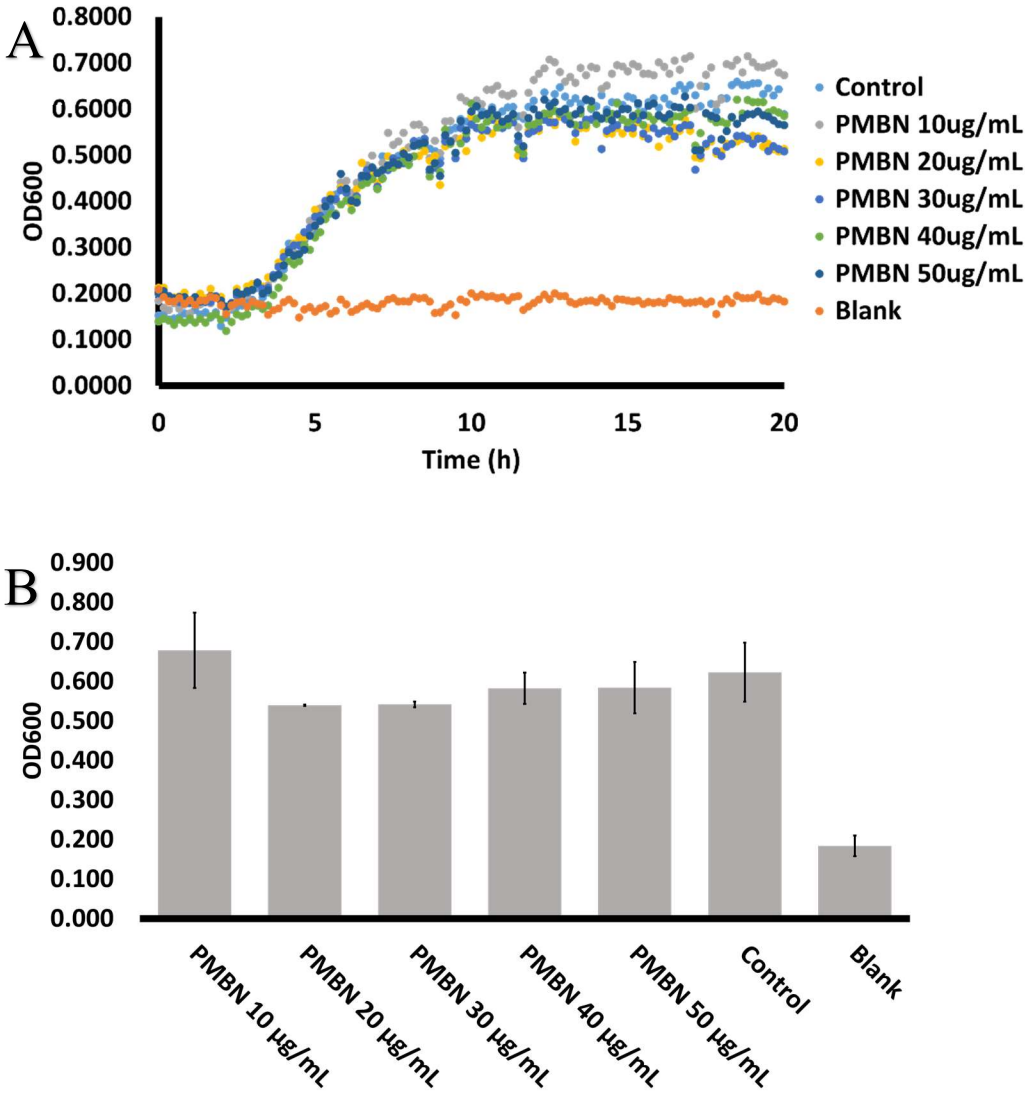

Figure 26. A) Growth curve of *E. coli* cells treated with PMBN and measured by absorbance. B) Averages acquired from 12-20 h with error bars. Statistical analysis showed no significant difference between the control and 50 µg/mL PMBN, indicating that these concentrations are not likely capable of limiting cellular growth.

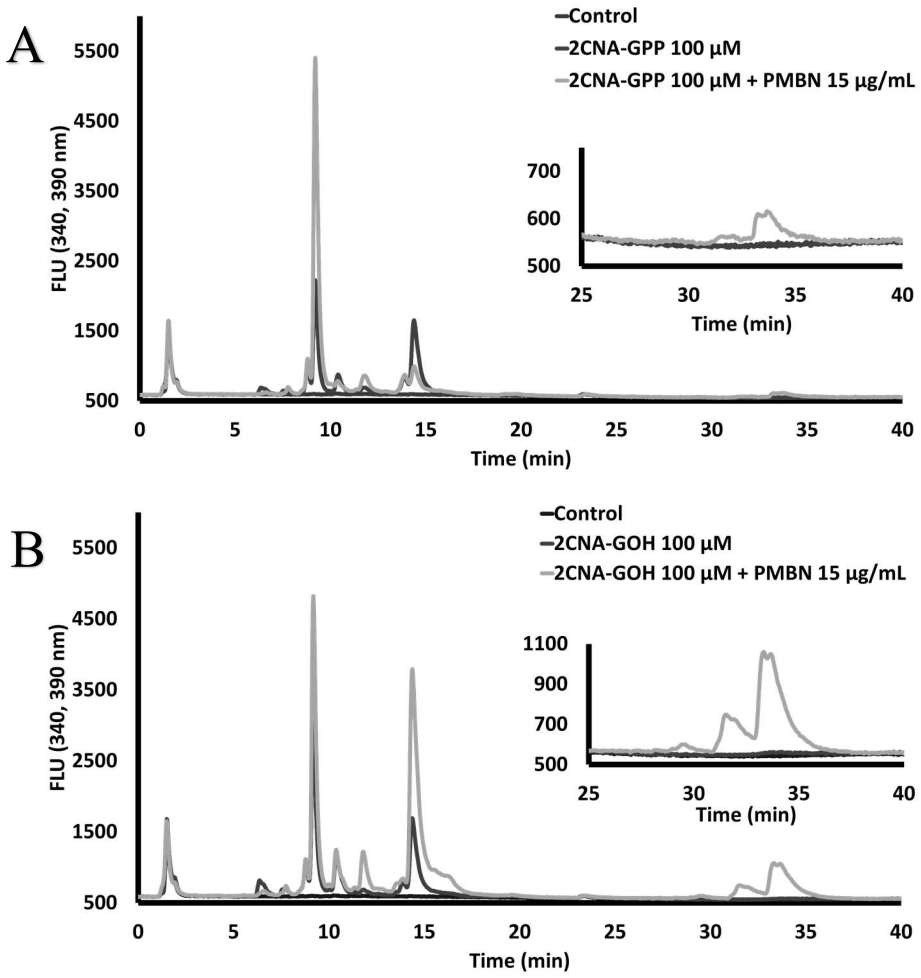

Figure 27. Comparison of cells treated with A) 100 µM 2CNA-GPP or B) 100 µM 2CNA-GOH with and without PMBN. Total protein content was adjusted to 1 mg/mL and 20 µL of each sample was injected for HPLC analysis. Cells treated with PMBN have better labeling for hydrophobic and hydrophilic products as observed by relative peak height as well as the number of products. The data presented is from a single replicate, however is representative of an observed trend.

As mentioned, PMBN concentrations were tested in a gradient to determine an optimal concentration for use. Initially, 0.3, 3, and 30 µg/mL were measured exclusively (Figure 28), however concentrations between 3 and 30 µg/mL were examined more closely (Figure 29). Prior to re-examination of concentrations closer to 30 µg/mL, we chose to utilize 30 µg/mL exclusively; this was later changed to 15 µg/mL due to the fact

that at this lower concentration, three distinct products in the hydrophobic region between roughly 30 and 35 min were still visible.

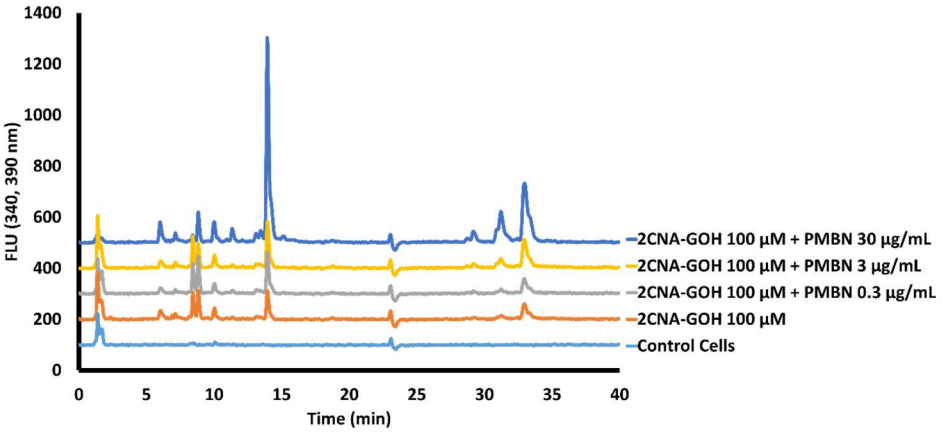

Figure 28. Comparison of cells treated with 100 µM 2CNA-GOH and varying concentrations of PMBN. With 30 µg/mL PMBN, labeled peaks are larger relative to other examined concentrations as well as cells treated with only 2CNA-GOH, indicating improved labeling. This experiment led to further examination of PMBN concentrations closer to 30 µg/mL.

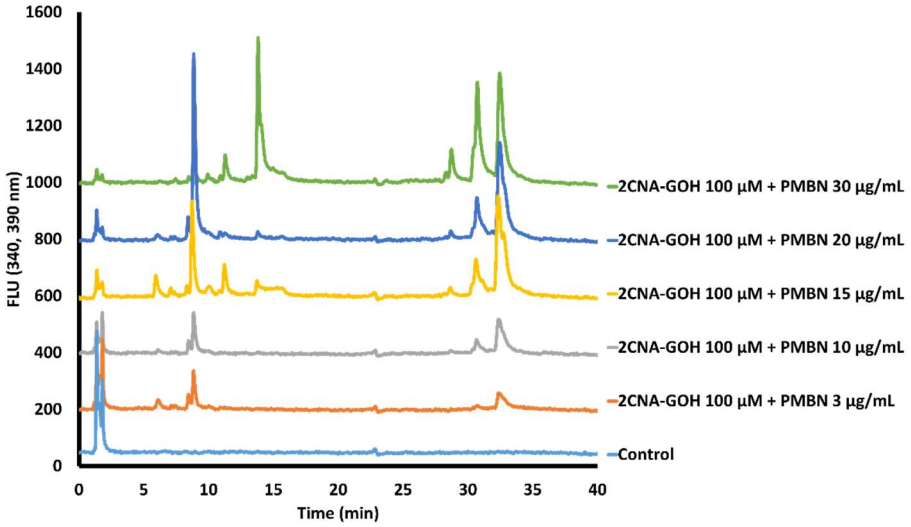

Figure 29. Comparison of cells treated with 100 µM 2CNA-GOH and varying concentrations of PMBN from 3 to 30 µg/mL. With a minimum of 15 µg/mL PMBN, labeled peaks are larger, indicating improved labeling. The data presented is from a single replicate, however is representative of an observed trend.

Table 5. Percent relative increases of samples treated with varying concentrations PMBN relative to a sample treated with 3 µg/mL PMBN at selected retention times. The selected retention times have been hypothesized to be potential BPP or BP products. Relative to 3 µg/mL PMBN, 15 µg/mL PMBN is the lowest concentration that shows improved product formation at these points.

PMBN Concentration (µg/mL)	Integrated area at 37 min	% Increase Relative to PMBN 3 µg/mL (%)	Integrated area at 38.8 min	% Increase Relative to PMBN 3 µg/mL (%)
3	782	-	4732.9	-
10	3358.7	76.72	8866.6	46.62
15	9431.9	91.71	25439.4	81.40
20	9195	91.50	24973.3	81.05
30	20919.3	96.26	20985.4	77.45

Obtained data demonstrates that higher concentrations of PMBN show better uptake and incorporation of 2CNA-GOH. When we analyzed PMBN concentrations closer to 30 µg/mL, cell samples with 15, 20, and 30 µg/mL PMBN showed similar peak heights with hydrophobic products (Table 5). The most noticeable difference is at ~14 min where the 30 µg/mL PMBN sample demonstrates a significantly higher peak. This peak lines up with 2CNA-GOH standards and we have interpreted this to be a possible maximum uptake of the analogue. Due to increased interest in hydrophobic products, we chose to mainly utilize 15 µg/mL PMBN as the product formation at this concentration was roughly comparable to that of higher concentrations.

3.2.4: Cellular Labeling of Isoprenoid-Linked Pathways Improves over Time

To optimize the time required for cell growth in regards to product formation, time point studies were conducted. We chose to examine cells every 4 h over a period of 24 h. Time point samples show a marked increase in HPLC peaks in the hydrophobic region the longer cells were allowed to grow in the presence of a fluorescent analogue (Figure 30). This effect plateaued by 18 h and remained comparable at later time points. This may be partly due to the health of the culture as cells transition from the stationary

phase to death. It should be noted that total protein content was not taken into consideration for analysis of the 4 h time point due to limitations from cell pellet size and a low total protein concentration; however, all other samples were adjusted.

We have further hypothesized that analogue incorporation is maximized when cell density is higher. Experiments exploring this hypothesis included incubating a turbid culture 2CNA-GOH for a minimum of 1 h; peaks with a higher retention time were not observed (Figure 31). We interpreted this to suggest one of two things: that either cells need to be capable of dividing in order to incorporate our analogues, or that an extended period of time is required for analogues to permeate the cell membrane and be incorporated into biosynthetic pathways. This is further supported by the limited number of peaks present in earlier time points in the 24 h study.

Studies also focused on eliminating the possibility that free proteins from natural cell death in the growth media are forming products. While preliminary results suggested this is unlikely, this argument offers another explanation as to why peak height increases over time; as cells lyse, more proteins become available in the growth media that may utilize or metabolize fluorescent substrates.

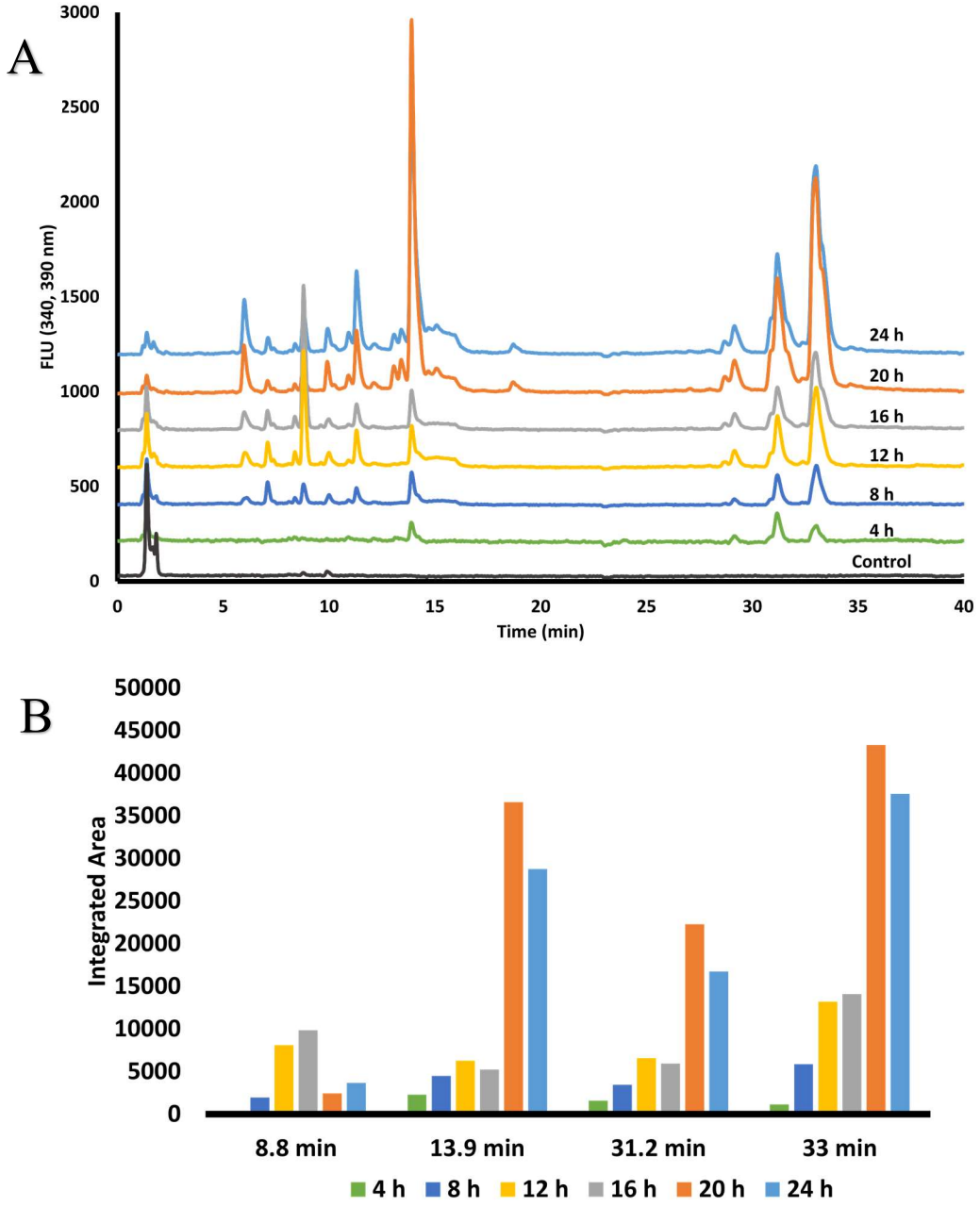

Figure 30. Comparison of cells treated with 100 µM 2CNA-GOH and 30 µg/mL PMBN sampled every 4 h for 24 h. Total protein content was matched to 1 mg/mL for all samples except for the 4 h sample due to limited cell pellet size; this sample had a total protein concentration of roughly 0.5 mg/mL. A) Chromatograms of each sample including a control. B) Integrated areas of each sample at selected retention times. The 13.9 min retention time was selected because this is commonly the retention time for 2CNA-GOH. 8.8 min is intended to be representative of hydrophilic peaks. Both 31.2 and 33 min retention times are considered peaks of interest due to expectation that these are either BP or BPP products. The data presented is from a single replicate, however is representative of an observed trend.

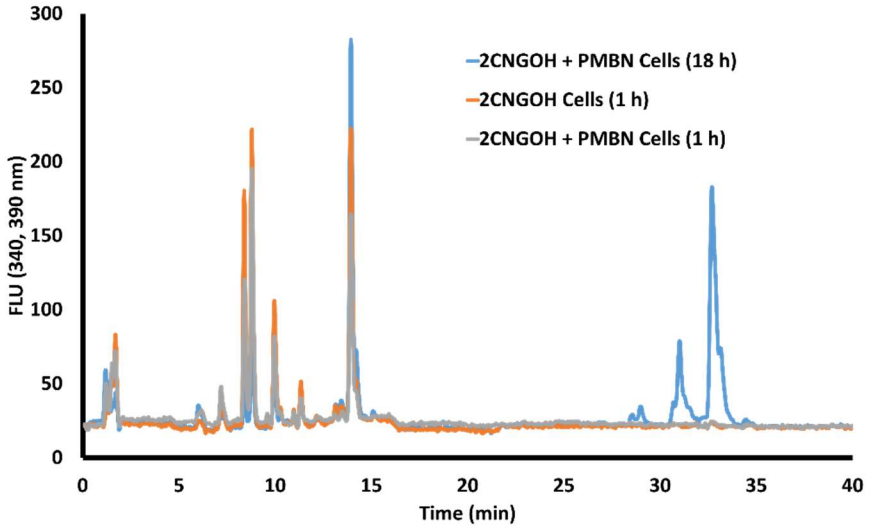

Figure 31. Comparison of cells grown in fluorescent analogue for 18 h versus grown and incubated in analogue for an hour. The presence of PMBN does not appear to influence the formation of hydrophobic compounds with short incubation periods.

3.3: Verification of Analogue Uptake

Based on the presented chromatogram data, we believed that analogues were not only entering cells but also being utilized. However, we had to consider the possibility that analogues were not entering cells, merely being modified by enzymes from lysed cells in the growth media during incubation. We therefore set up a series of experiments for verification of cellular uptake. Figure 32 describes the general methods involved in these experiments.

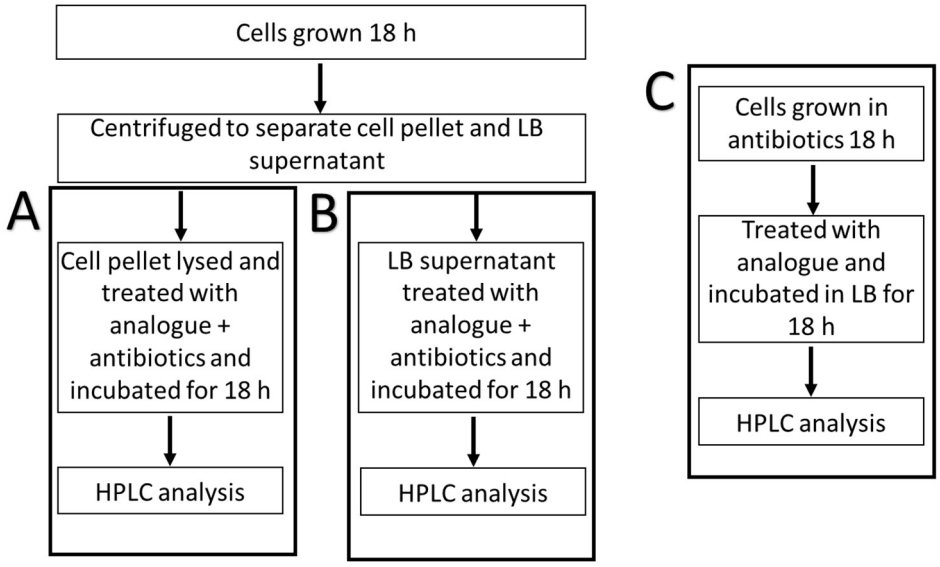

Figure 32. General methods for verification of analogue uptake. A) Method for lysate studies involving freshly lysed cell material. B) Method for labeled supernatant, shown in later figures as "grown LB". C) Method for "dead cell material" verification involving the generation of lysed cellular material in LB. Antibiotics used were 0.1 μg/mL PMB and 25 μg/mL chloramphenicol. All samples were filtered prior to HPLC analysis.

The first approach was to incubate freshly-lysed cellular material with our FPP analogues and monitor changes by HPLC. Initial attempts at this suggested that some cells may remain intact following lysis by sonication, so we employed the use of antibiotics to limit further growth. This was to ensure that any modifications made to analogues were from free enzymes and not intact cells. This set of experiments was termed "lysate studies" and are defined as experiments that utilize lysed cellular material from *E. coli* cells that have been grown to a high turbidity over 18 h without any added substances, including analogues or membrane permeabilizers. The antibiotics used to prevent further cellular growth include chloramphenicol and PMB. These antibiotics were selected based on their different mechanisms of action; PMB interactions with LPS to disrupt the cell membrane while chloramphenicol disrupts ribosome activity.[40] MICs were conducted and are displayed in Figure 33. Based on the literature, expected MIC values for chloramphenicol and PMB were 2 μg/mL and 0.5μg/mL, respectively.[54, 57]

Note that the PMB MIC curve from section 3.2.2 is presented again for ease of reference. The MIC for chloramphenicol is calculated to be roughly 7 μg/mL and the MIC for PMB is roughly 0.6 μg/mL. For these studies, we chose to use 25 μg/mL chloramphenicol and 0.1 μg/mL PMB in conjunction.

Lysate from unlabeled cells was treated with either 2CNA-GOH or 2CNA-GPP in lysis buffer post-sonication (Figure 34, Table 6). Prior to treatment, lysate was matched for total protein content via Bradford Assay and diluted in lysis buffer mentioned antibiotics. Following incubation, samples were streaked on agar plates to ensure that undesired cell growth did not occur. There was no apparent difference between these two samples after 18 h, and there were few peaks present after ~16 min via HPLC (Table 6). The peaks that were present in each treated lysate sample represent less than 1% of the total fluorescent products for each sample. We hypothesize this to mean that while free enzymes may still be active and utilize the analogues, UppS is likely not active enough to produce large quantities of fluorescently labeled BPP. It should be noted that in this sample, the added 2CNA-GPP seems to disappear (7 min), however the alcohol peak is highly prominent (~14 min). This may suggest either a modification or consumption of this analogue.

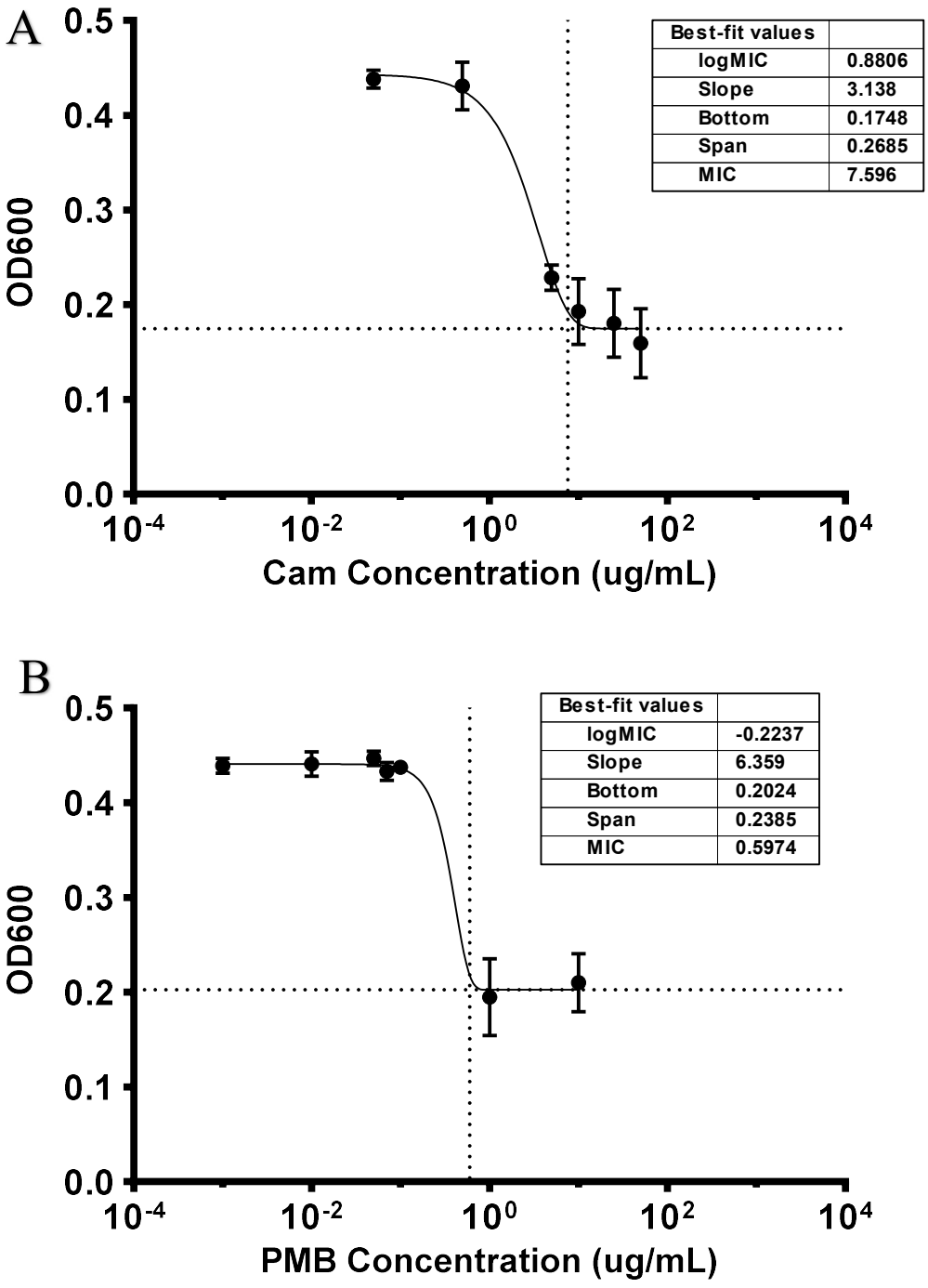

Figure 33. MIC curves of A) chloramphenicol, displayed as Cam, and B) PMB on *E. coli* strain MAJ427. In both figures, the slope of the calculated curve, the lowest measured OD (bottom), and the difference between the lowest and highest measured ODs (span) are displayed. The calculated MIC for chloramphenicol is roughly 7 µg/mL and the MIC for PMB is roughly 0.6 µg/mL utilizing this *E. coli* strain.

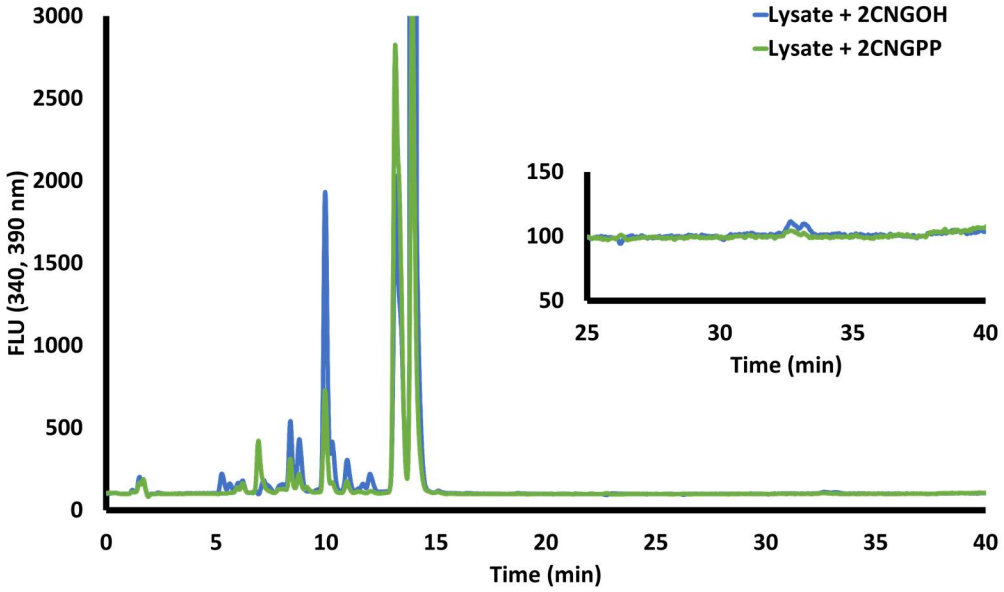

Figure 34. Comparison of lysed cell material treated with either 2CNA-GOH or 2CNA-GPP. Though peaks other than the fluorescent analogues themselves are visible, there are no significant peaks in the hydrophobic region suggesting that 2CNA-BP was not produced in large quantities, if at all.

Table 6. Integrations of HPLC peaks from lysate treated with 2CNA-GPP or 2CNA-GOH. Peaks under 2 min have not been integrated as they are flow-through and not representative of actual fluorescent products.

Lysate + GPP				Lysate + GOH			
Peak	Retention time (min)	Integrated Area	% of Total Integrated Area (%)	Peak	Retention time (min)	Integrated Area	% of Total Integrated Area (%)
1	6.925	4945.5	4.004	1	5.258	1464.5	0.772
2	8.367	2290.1	1.854	2	6	554.4	0.292
3	8.766	1514.8	1.226	3	6.195	826.9	0.436
4	9.952	7463.9	6.043	4	7.154	2041	1.076
5	10.945	936.1	0.758	5	8.024	1052.5	0.555
6	13.149	58063.7	47.011	6	8.376	4907.4	2.587
7	13.92	47363.6	38.348	7	8.781	4420.7	2.33
8	26.394	933.2	0.756	8	9.96	21711.4	11.445
				9	10.277	3594.1	1.895
				10	10.96	2577	1.358
				11	12	1636.3	0.863
				12	13.162	40840.7	21.528
				13	14.108	102557.7	54.061
				15	25.392	426.6	0.225
				16	26.42	920.4	0.485

Because our initial lysate study did not take into consideration incubation in the growth media itself, we explored utilizing chloramphenicol and PMB as a way to kill cells and produce lysed cell material in LB (Figure 35, Table 7). We termed these "dead cell material" cultures based on the cultivation of lysed, dead cellular material. Our approach once again utilized 25 μg/mL chloramphenicol and 0.1 μg/mL PMB, similar to the lysate studies. Cultures were inoculated with significantly less bacteria compared to our standard cell labeling protocol and incubated at 37 °C with the aforementioned antibiotics present; the amount of cells present was more comparable to an MIC study to ensure that the added amount of antibiotics could fully kill cells. After 18 h, cultures were treated with either 2CNA-GOH or 2CNA-GPP and incubated further. Due to limited or no cellular growth, analysis was performed straight on HPLC after filtration and compared to an LB blank. Overall, there were no noteworthy peaks past those of the analogues themselves. This suggests that either free proteins in the LB are not responsible for observed peaks in labeled cell cultures, not enough proteins were present, or present proteins denatured prior to treatment with fluorescent analogues. Another possibility is that there was not enough cellular material injected on the HPLC to show the presence of fluorescent products. Finally, it should be noted that degradation of the analogues was not observed in the growth media, demonstrating that these compounds are not likely to naturally degrade in these conditions.

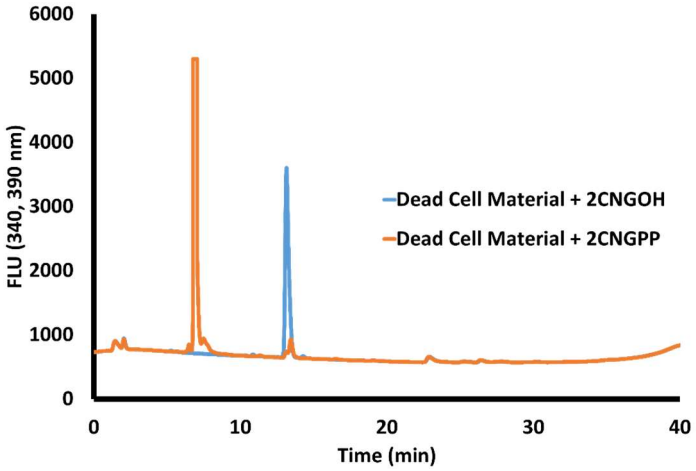

Figure 35. Comparison of dead cell material treated with either 2CNA-GOH or 2CNA-GPP. In both cultures, peaks past those belonging to the initial fluorescent material were not observed.

Table 7. Integrations of HPLC peaks from lysate dead cell material treated with 2CNA-GPP or 2CNA-GOH. Peaks under 2 min have not been integrated as they are flow-through and not representative of actual fluorescent products. Similarly, the peak at 23 min was not integrated due to its presence in control and blank samples.

Dead Cell Mat. + GPP				Dead Cell Mat. + GOH			
Peak	Retention time (min)	Integrated Area	% of Total Integrated Area (%)	Peak	Retention time (min)	Integrated Area	% of Total Integrated Area (%)
1	6.499	987.8	0.982	1	13.147	51140.9	100
2	7.045	87849.8	87.374				
3	7.487	5779.6	5.748				
4	13.131	1152.7	1.146				
5	13.438	4775.1	4.749				

Our final approach utilized the LB supernatant of an already-grown cell culture, as we believed that dead cellular material may already be present. Also, we suspected that the potentially limited cell material from the previous experiment was not sufficient for examination of any present enzymes in the growth media. LB acquired from a previously mentioned unlabeled lysate culture was treated with chloramphenicol, PMB, and fluorescent analogues for 18 h. The LB was obtained following the initial "soft spin" in the analysis preparation process. It was hypothesized that viable cells may still be

present in the LB supernatant, therefore antibiotics were added as a precaution. HPLC analysis shows that this culture was similar to the dead cell material cultures; the only peaks present are those of the analogues themselves (Figure 36, Table 8).

Other approaches for verification were attempted including testing the absorbance of a mixture of resuspended cells at 340 nm, as well as lysed cells at the same wavelenght, however these were not conclusive. We believe that these approaches have inherent flaws due to the heterogenous natures of the mixtures, as well as the fact that we are currently unaware of exactly how much analogue is being brought into cells; it is possible that this concentration is below a reasonable limit of detection with available instruments.

This series of studies strongly suggests that our fluorescent analogues are, in fact, not only permeating the cellular membrane of *E. coli*, but also getting incorporated into appropriate pathways. This is opposed to the possibility that fluorescent product formation is occurring from cellular material that has been ejected from dead cells in the growth culture.

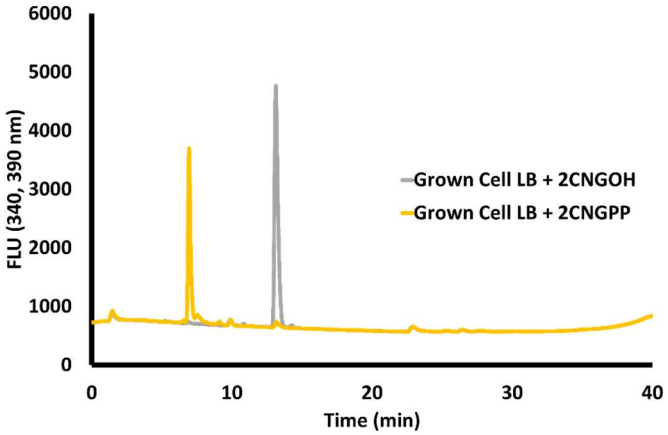

Figure 36. Comparison of "grown LB" treated with either 2CNA-GOH or 2CNA-GPP. Similarly to the lysate culture samples, there were no peaks present other than those belonging to the analogues themselves.

Table 8. Integrations of HPLC peaks from recovered LB supernatant (grown LB) treated with 2CNA-GPP or 2CNA-GOH. Peaks under 2 min have not been integrated as they are flow-through and not representative of actual fluorescent products. Similarly, the peak at 23 min was not integrated due to its presence in control and blank samples.

Grown LB + GPP				Grown LB + GOH			
Peak	Retention time (min)	Integrated Area	% of Total Integrated Area (%)	Peak	Retention time (min)	Integrated Area	% of Total Integrated Area (%)
1	6.54	355.9	0.786	1	9.876	1646.3	2.243
2	6.943	37158.5	82.06	2	13.125	71043.4	96.784
3	7.529	3519	7.771	3	14.25	714.4	0.973
4	9.097	729.4	1.611				
5	9.908	1441.5	3.183				
6	13.159	2077.9	4.589				

3.4: Characterization of Fluorescent Products

3.4.1: Separation and Analysis of Cellular Fractions

To better understand what types of compounds might be labeled and to assist with the identification of fluorescent products, subfractionation on labeled cellular material was performed. We expected hydrophobic compounds, such as BP and BPP, to be in the

inner membrane, and residual analogue to be located in the cytoplasm. Analysis of the cytosolic and membrane fractions of the cell indicates that fluorescent, hydrophobic products are located in the membrane fraction (Figure 37, Table 9). This agrees with our suggestion that these products are fluorescently labeled BP and BPP products, as they are embedded in the membrane of *E. coli*. Hydrophilic compounds with shorter retention times appear to be most prominent in the cytosolic fraction, including 2CNA-GOH and possibly 2CNA-GPP. This suggests that these compounds are taken into the cell and may reside within the cytosol before incorporation.

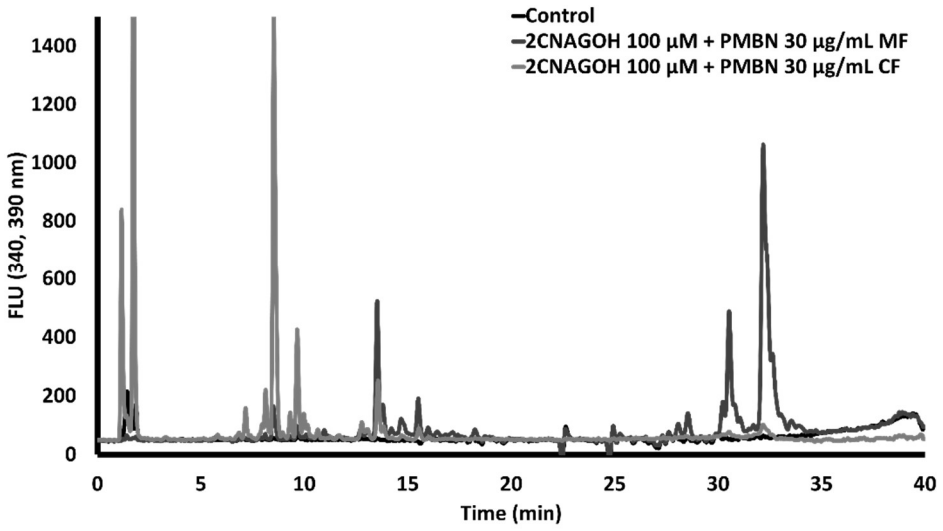

Figure 37. Comparison of membrane and cytoplasmic components separated by selective solubility using 0.1% Triton. Hydrophobic peaks appeared exclusively in the membrane fraction while a majority of hydrophilic peaks were present in the cytoplasmic fraction. Total protein content was not matched for these samples.

Table 9. Integrations of peaks from HPLC examining tested cytosolic and membrane fractions. A) The majority of peaks present in the cytosolic fraction (CF) sample are hydrophilic in nature (retention time ≤ 25 min), which makes sense for this sample. The largest peak occurs at 8.5 min and represents 57% of the total products in the CF. Further, while products are present at 31 and 32 min, these comprise less than 6% of the overall integrated area. B) Fewer peaks are present in the membrane fraction (MF) sample compared to the CF, however the most prominent peaks are hydrophobic (retention time ≥ 25 min) and comprise 75% of the total products in the MF.

Cytosolic Fraction

Peak	Retention time (min)	Integrated Area	% of Total Integrated Area (%)
1	7.16	876.8	3.57
2	8.13	1560.8	6.36
3	8.52	13999.7	57.07
4	9.66	3218.4	13.12
5	12.78	1235.3	5.04
6	13.56	2335.4	9.52
7	31.04	474.2	1.93
8	32.16	829.8	3.38

Membrane Fraction

Peak	Retention time (min)	Integrated Area	% of Total Integrated Area (%)
1	8.49	983.4	2.42
2	13.52	5421.3	13.36
3	14.67	837.5	2.06
4	15.51	2783.1	6.86
5	30.53	7814.3	19.26
6	32.18	22737	56.04

3.4.2: Mass Spectrometry of Isolated Products

Products acquired via HPLC isolation were analyzed by MS and the analysis can be seen below (Figures 38 and 39). It is suspected that the peak originally at 29 minutes is a cis-7 2CNA-BPP with an associated potassium ion, however this is not the appropriate retention time for that product based on standards. As for the 31 min isolated peak, an exact structure has not been proposed that matches the mass; the presented

structure is 2 m/z units off. Again, the retention time does not match the structure compared to standards. More work is required to better identify these structures.

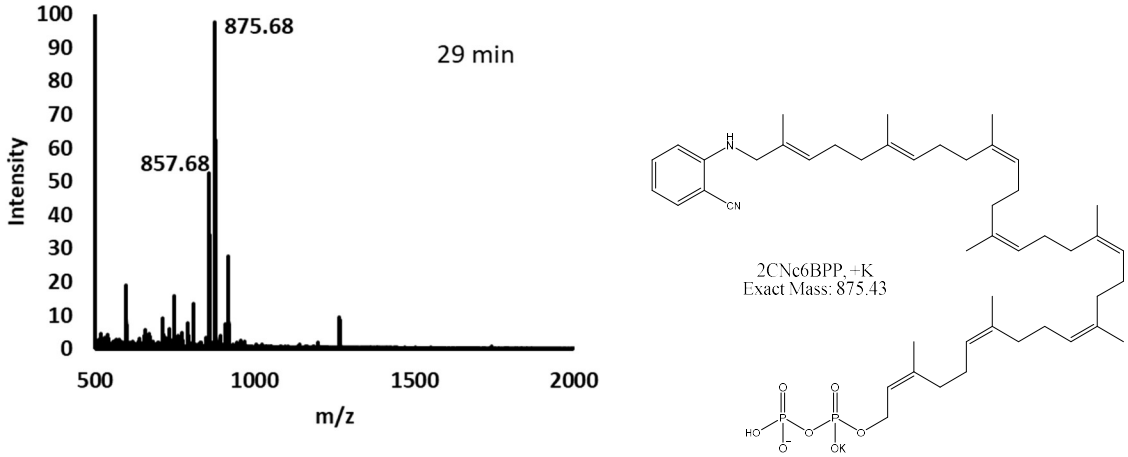

Figure 38. MS of products isolated from cells treated with 100 µM 2CNA-GOH and 15 µg/mL PMBN, as well as structure of a possible product. This sample was acquired through HPLC isolation and had a retention time of 29 min.

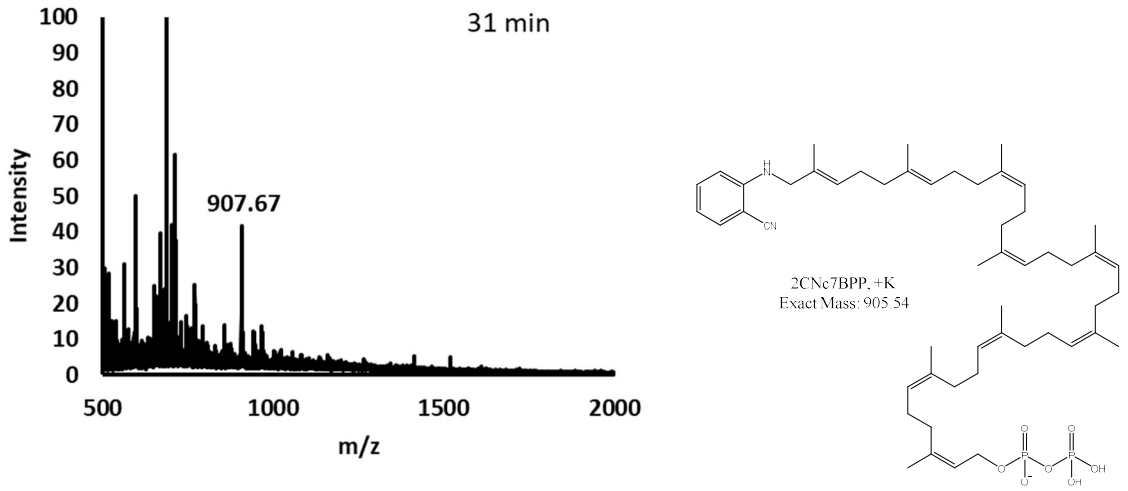

Figure 39. MS of products isolated from cells treated with 100 µM 2CNA-GOH and 15 µg/mL PMBN, as well as structure of a possible product. This sample was acquired through HPLC isolation and had a retention time of 31 min.

CHAPTER FOUR: DISCUSSION & FUTURE DIRECTIONS

4.1: Overview of Presented Research

The work described here details the application of a platform for the discovery of the function of genes in bacterial isoprenoid-linked pathways. Former techniques to track glycan pathways in eukaryotes have often focused on the utilization of chemically-modified sugars.[46] However, prokaryotes harness the metabolic capacity to incorporate and modify a larger array of sugars than eukaryotes do, which makes this yet another challenging approach. This work instead utilizes fluorescent isoprenoid analogues such as 2CNA-GPP and 2CNA-GOH to indirectly monitor glycan formation. While similar work has been conducted using FPP analogues in eukaryotes,[47] this platform has not previously been reported in bacteria and is significant for the understanding of associated metabolic pathways such as polysaccharide biosynthesis. Polysaccharides in bacteria play countless roles including membrane development, biofilm formation, cell recognition, and survival.[58] Other polysaccharides have unique features, such as the *Caulobacter crescentus* holdfast polysaccharide, which has remarkably strong adhesive properties.[59-60] Undoubtedly, countless other polysaccharides with remarkable and useful properties have yet to be discovered. Further, the identification and understanding of proteins responsible for forming polysaccharides associated with biofilm formation could ultimately result in novel antibiotic targets.

To accomplish the goal of better understanding these pathways, a protocol was first devised to label bacterial cells with fluorescent isoprenoid tags. Once this was accomplished, several variables including incubation time and analogue concentration

were examined and optimized; membrane permeabilizers such as antibiotics and chelating agents were also considered and incorporated when appropriate. We also utilized rescue studies to examine whether or not synthesized FPP analogues can pass through a bacterial cell membrane and be incorporated into isoprenoid pathways. While we have seen little success with our fluorescent analogues, it is possible that the bacterial cells cannot utilize isoprenoids larger than IPP to compensate for the effects of fosmidomycin.

A restraint to our current rescue studies protocol involves the use of fosmidomycin rather than a FPP synthase (FppS) inhibitor. This may be more appropriate for these studies due to the ability to examine the impacts of FPP rather than IPP. Because IPP is required for the formation of BPP, limiting this pathway demands the addition of exogenous IPP to ensure that cells don't fully die. However, cells may also be capable of forming FPP from the exogenous IPP, making it challenging to examine the impacts of added FPP or FPP analogues. While drugs exist that can inhibit FppS in eukaryotes, limited options are available for prokaryotes, limiting this experiment to the utilization of fosmidomycin.[61-62]

As mentioned in section 3.2.2, complications arose during rescue experiments. We originally assumed that fosmidomycin was degrading at 37 °C over time, however kinetics conducted via ^{1}HNMR showed this was not likely the case. Due to the consistency of growth across all samples treated with the antibiotic, we also concluded that spontaneous resistance was not the cause of delayed growth. Upon further examination at past literature, we discovered that the gene fsr, fosmidomycin resistance

protein, was likely activated and either functioned as a pump directly or working with another mechanism to export fosmidomycin.[63] Therefore, further work is needed to obtain a definitive answer regarding whether or not exogenous IPP can rescue fosmidomycin afflicted bacterial cells. This may include excision of any genes related to fsr.

4.2: Characterization of Isoprenoid-Linked Compounds

Though some progress was made, characterization of HPLC-visualized fluorescent isoprenoid compounds is currently ongoing and more work is required. First, the likely overlap of hydrophobic products utilizing current analytical methods is problematic. To remedy this, a new HPLC method will need to be developed that will be able to better separate larger, hydrophobic compounds. This may involve examining other solvents or utilization of an isocratic method. Second, it is currently unknown if our fluorescent analogues can be incorporated into pathways associated with the formation of quinones, or if the presence of an analogue influences the final length of a formed BP. It is currently hypothesized that our analogues likely are incorporated into OPP, the precursor of many quinone side chains, but incorporation of a fluorescent analogue may prevent the addition of these side chains as the bond formation occurs at the end of the compound where the fluorescent moiety is located. As a majority of quinones are associated with electron transfer within cells, examination into these impacts may better illuminate these pathways and the full range of their impacts.

4.3: Applications of Fluorescently-Labeled Isoprenoids

The long-term goal of this project is the development of a platform to more readily study proteins associated with isoprenoid or glycan pathways in bacteria. Currently, homology studies are the fastest way to propose the functions of newly discovered enzymes, but these studies are not always accurate. Following these often computational studies, verification of enzyme function is still required; this involves proper identification of a substrate as well as optimizing enzyme conditions. The Troutman lab has applied this approach to the understanding of both the capsular polysaccharide A pathway in *Bacterioides fragilis*,[27] and the colanic acid pathway in *E. coli* (unpublished). However, by creating genetic knockouts and examining the chemical composition of the built-up material, we may be able to more quickly assign functions for enzymes in isoprenoid-linked pathways.

The first enzyme we would like to identify with this platform is a kinase, likely responsible for the conversion of farnesol to FPP within cells. While currently unknown, we hypothesize that there is a kinase likely present in the cytoplasm that is capable of converting 2CNA-GOH to 2CNA-GPP. Recent research has suggested that *E. coli* possesses endogenous phosphatases capable of converting FPP to FOH.[64] It is therefore plausible that a kinase and regulatory mechanism exists to complement this process. We have shown in the past that the 2CNA analogue as well as others not discussed are capable of being utilized as a substrate for UppS.[27, 36] Assuming similar substrate specificity, it is plausible that a potential kinase would be able to phosphorylate 2CNA-GOH and enable its incorporation into isoprenoid pathways.

Another application of this platform not previously mentioned is the potential quantification of common pools of BP. Several papers published by the Young lab have proposed the concept of a limited common pool of BP in bacteria. By creating genetic knockouts in various polysaccharide pathways, they noticed similar morphological changes whenever a buildup of polysaccharide intermediate was expected, regardless of the pathway. Their work has examined pathways associated with O-antigen, enterobacterial common antigen, and colanic acid, and has led them to the belief that this common, constant pool can be sequestered by a dysfunctional pathway.[3, 32, 65] This may result in issues with limited formation of peptidoglycan and ultimately cause the observed morphological changes. While this platform cannot currently and unequivocally determine the total amount of BP present, with better separation it may be possible to verify their sequestration hypothesis. It may be possible to quantify the common BP pool by first quantifying the amount of fluorescent analogue that enters the cell. Next, identification of BP-linked products combined with known molar quantities of standards may give an estimation as to how much BP is present. If applied to a strain that is expected to demonstrate morphological deformities, it could be possible.

4.3.2: Application of Presented Methods toward Genetic Mutants

Further applications for this platform have been attempted with little success and therefore the data is not presented. In this and the next section, however, complications concerning these applications will be discussed briefly. These applications include the examination of isoprenoid-linked glycan intermediates in the colanic acid pathway and identification of the function of either the Tlc2 or Tlc3 protein from *Rickettsia*

prowazekki. Using this pathway, it is unlikely that functions of both Tlc2 and Tlc3 will be elucidated as it is currently hypothesized that only one acts as an isoprenoid transporter.

Following our initial cellular labeling experiments, we decided to examine differences that may occur between genetic knockouts in a polysaccharide biosynthetic pathway; to this end, we chose to compare colanic acid knockouts. Preliminary work has been conducted on colanic acid mutants acquired courtesy of the Young lab at the University of Arkansas for Medical Sciences[32] with limited success (data not shown). Colanic acid mutants were anticipated to show differences in hydrophobic regions, representative of polysaccharide intermediates from the colanic acid pathway. We observed that the overall labeling of the genetic knockouts was less successful than in that of the wildtype. In past work with genetic mutants of isoprenoid pathways, the Young lab has observed morphological changes occurring whenever a buildup of an isoprenoid-linked intermediate is anticipated, therefore we expected to see somewhat similar results between all knockouts. It is possible that these peaks cannot be reliably associated with isoprenoid-linked glycans, however, as these peaks have not yet been fully characterized, this is not certain.

4.3.3: Application of Presented Methods toward Protein Identification

Eukaryotes are known to utilize the mevalonate pathway to synthesize needed IPP.[13] Prokaryotes typically use the non-mevalonate pathway, though some exceptions exist.[2, 66] *Rickettisa prowazekki*, however, is not known to employ either pathway yet retains enzymes for modifying and condensing isoprenoids, implying that exogenous

isoprenoids must be brought into the bacteria in order to satisfy metabolic requirements.[67] Because of this, researchers have hypothesized the existence of an isoprenoid transport protein capable of actively transporting isoprenoids across the cell membrane.

As mentioned in section 1.6, the Tlc proteins in *Rickettsia prowazekki* are all believed to function as some form of transport for various types of compounds. Tlc1, Tlc4, and Tlc5 have all been identified, but the functions of Tlc2 and Tlc3 are currently unknown. It is hypothesized that one of these is likely associated with isoprenoid transport, and we explored this utilizing our 2CNA-GPP analogue. Based on preliminary HPLC results (data not shown), we currently believe that Tlc3 is more likely to be involved in isoprenoid uptake compared to Tlc2. However, we also believe that these results are not fully conclusive and that the use of a modified rescue study may be more appropriate.

Complicating variables demand that a different approach be used than what we have shown in this work with current protocols. For example, *E. coli* cells with transformed plasmids to overproduce the Tlc proteins were used, requiring the use of isopropyl β-D-1-thiogalactopyranoside (IPTG). However, preliminary studies suggest that excess IPTG results in diminished cellular growth. We believe that the amount of IPTG added needs to be optimized to increase the abundance of the Tlc proteins, but also not significantly diminish overall growth capacity. Our initial studies focused on using protocols similar to rescue studies with limited results, and we suggest that traditional methods involving plating cells and measuring colony forming units (CFUs) would be more appropriate. Finally, further studies should focus primarily on examining the

transport of IPP rather than FPP or FPP analogues as it is the simplest isoprenoid. We anticipate that these approaches will more definitively identify the isoprenoid transporter. Once identified, we plan on utilizing the protein to improve uptake of our fluorescent analogues to further improve the platform presented in this research.

REFERENCES

1. Siegrist, M. S.; Swarts, B. M.; Fox, D. M.; Lim, S. A.; Bertozzi, C. R., Illumination of growth, division and secretion by metabolic labeling of the bacterial cell surface. *FEMS Microbiol Rev* **2015,** *39* (2), 184-202.
2. Li, Y.; Wang, G., Strategies of isoprenoids production in engineered bacteria. *Journal of Applied Microbiology* **2016,** *121* (4), 932-940.
3. Jorgenson, M. A.; Kannan, S.; Laubacher, M. E.; Young, K. D., Dead-end intermediates in the enterobacterial common antigen pathway induce morphological defects in Escherichia coli by competing for undecaprenyl phosphate. *Mol Microbiol* **2016,** *100* (1), 1-14.
4. Jorgenson, M. A.; Young, K. D., Interrupting Biosynthesis of O Antigen or the Lipopolysaccharide Core Produces Morphological Defects in Escherichia coli by Sequestering Undecaprenyl Phosphate. *J Bacteriol* **2016,** *198* (22), 3070-3079.
5. Ajit Varki, R. C., Jeffery Esko, Hudson Freeze, Gerald Hart, Jamey Marth, *Essentials of Glycobiology*. Cold Springs Harbor Laboratory Press: Cold Spring Harbor, NY, 1999.
6. Kiessling, L. L.; Splain, R. A., Chemical Approaches to Glycobiology. In *Annual Review of Biochemistry, Vol 79*, Kornberg, R. D.; Raetz, C. R. H.; Rothman, J. E.; Thorner, J. W., Eds. Annual Reviews: Palo Alto, 2010; Vol. 79, pp 619-653.
7. Imperiali, B., METHODS IN ENZYMOLOGY Chemical Glycobiology Part A. Synthesis, Manipulation and Applications of Glycans PREFACE. In *Chemical Glycobiology, Pt a: Synthesis, Manipulation and Applications of Glycans*, Imperiali, B., Ed. Elsevier Academic Press Inc: San Diego, 2017; Vol. 597, pp XV-XIX.
8. Nothaft, H.; Szymanski, C. M., Bacterial Protein N-Glycosylation: New Perspectives and Applications. *Journal of Biological Chemistry* **2013,** *288* (10), 6912-6920.
9. Jones, M. B.; Rosenberg, J. N.; Betenbaugh, M. J.; Krag, S. S., Structure and synthesis of polyisoprenoids used in N-glycosylation across the three domains of life. *Biochim. Biophys. Acta-Gen. Subj.* **2009,** *1790* (6), 485-494.
10. Gerin, I.; Ury, B.; Breloy, I.; Bouchet-Seraphin, C.; Bolsee, J.; Halbout, M.; Graff, J.; Vertommen, D.; Muccioli, G. G.; Seta, N.; Cuisset, J. M.; Dabaj, I.; Quijano-Roy, S.; Grahn, A.; Van Schaftingen, E.; Bommer, G. T., ISPD produces CDP-ribitol used by FKTN and FKRP to transfer ribitol phosphate onto alpha-dystroglycan. *Nat. Commun.* **2016,** *7*, 15.
11. Wolfe, L. A.; Morava, E.; He, M.; Vockley, J.; Gibson, K. M., Heritable disorders in the metabolism of the dolichols: A bridge from sterol biosynthesis to molecular glycosylation. *Am. J. Med. Genet. C* **2012,** *160C* (4), 322-328.
12. Hoffmann, R.; Grabinska, K.; Guan, Z. Q.; Sessa, W. C.; Neiman, A. M., Long-Chain Polyprenols Promote Spore Wall Formation in Saccharomyces cerevisiae. *Genetics* **2017,** *207* (4), 1371-1386.
13. Leon, A.; Liu, L.; Yang, Y.; Hudock, M. P.; Hall, P.; Yin, F. L.; Studer, D.; Puan, K. J.; Morita, C. T.; Oldfield, E., Isoprenoid biosynthesis as a drug target: Bisphosphonate inhibition of Escherichia coli K12 growth and synergistic effects of fosmidomycin. *J. Med. Chem.* **2006,** *49* (25), 7331-7341.

14. Cox, G. B.; Newton, N. A.; Gibson, F.; Snoswell, A. M.; Hamilton, J. A., The function of ubiquinone in Escherichia coli. *Biochem J* **1970,** *117* (3), 551-62.
15. Aussel, L.; Pierrel, F.; Loiseau, L.; Lombard, M.; Fontecave, M.; Barras, F., Biosynthesis and physiology of coenzyme Q in bacteria. *Biochim. Biophys. Acta-Bioenerg.* **2014,** *1837* (7), 1004-1011.
16. Morishita, T.; Tamura, N.; Makino, T.; Kudo, S., Production of menaquinones by lactic acid bacteria. *J. Dairy Sci.* **1999,** *82* (9), 1897-1903.
17. Nowicka, B.; Kruk, J., Occurrence, biosynthesis and function of isoprenoid quinones. *Biochim. Biophys. Acta-Bioenerg.* **2010,** *1797* (8), 1587-1605.
18. El Ghachi, M.; Howe, N.; Huang, C. Y.; Olieric, V.; Warshamanage, R.; Touze, T.; Weichert, D.; Stansfeld, P. J.; Wang, M. T.; Kerff, F.; Caffrey, M., Crystal structure of undecaprenyl-pyrophosphate phosphatase and its role in peptidoglycan biosynthesis. *Nat. Commun.* **2018,** *9*, 13.
19. Hartley, M. D.; Larkin, A.; Imperiali, B., Chemoenzymatic synthesis of polyprenyl phosphates. *Bioorganic & Medicinal Chemistry* **2008,** *16* (9), 5149-5156.
20. Kalin, J. R.; Allen, C. M., CHARACTERIZATION OF UNDECAPRENOL KINASE FROM LACTOBACILLUS-PLANTARUM. *Biochimica Et Biophysica Acta* **1979,** *574* (1), 112-122.
21. Manat, G.; El Ghachi, M.; Auger, R.; Baouche, K.; Olatunji, S.; Kerff, F.; Touze, T.; Mengin-Lecreulx, D.; Bouhss, A., Membrane Topology and Biochemical Characterization of the Escherichia coli BacA Undecaprenyl-Pyrophosphate Phosphatase. *PLoS One* **2015,** *10* (11), 21.
22. Wang, Y.; Desai, J.; Zhang, Y. H.; Malwal, S. R.; Shin, C. J.; Feng, X. X.; Sun, H.; Liu, G. Z.; Guo, R. T.; Oldfield, E., Bacterial Cell Growth Inhibitors Targeting Undecaprenyl Diphosphate Synthase and Undecaprenyl Diphosphate Phosphatase. *ChemMedChem* **2016,** *11* (20), 2311-2319.
23. Cuthbertson, L.; Mainprize, I. L.; Naismith, J. H.; Whitfield, C., Pivotal Roles of the Outer Membrane Polysaccharide Export and Polysaccharide Copolymerase Protein Families in Export of Extracellular Polysaccharides in Gram-Negative Bacteria. *Microbiol. Mol. Biol. Rev.* **2009,** *73* (1), 155-+.
24. Baum, L. G., Developing a taste for sweets. *Immunity* **2002,** *16* (1), 5-8.
25. Pragani, R.; Seeberger, P. H., Total Synthesis of the Bacteroides fragilis Zwitterionic Polysaccharide A1 Repeating Unit. *J. Am. Chem. Soc.* **2011,** *133* (1), 102-107.
26. Mazmanian, S. K.; Kasper, D. L., The love-hate relationship between bacterial polysaccharides and the host immune system. *Nat. Rev. Immunol.* **2006,** *6* (11), 849-858.
27. Sharma, S.; Erickson, K. M.; Troutman, J. M., Complete Tetrasaccharide Repeat Unit Biosynthesis of the Immunomodulatory Bacteroides fragilis Capsular Polysaccharide A. *ACS Chem Biol* **2017,** *12* (1), 92-101.
28. Zhang, C. S.; Griffith, B. R.; Fu, Q.; Albermann, C.; Fu, X.; Lee, I. K.; Li, L. J.; Thorson, J. S., Exploiting the reversibility of natural product glycosyltransferase-catalyzed reactions. *Science* **2006,** *313* (5791), 1291-1294.
29. Agard, N. J.; Bertozzi, C. R., Chemical Approaches To Perturb, Profile, and Perceive Glycans. *Accounts Chem. Res.* **2009,** *42* (6), 788-797.

30. Lowe, J. B.; Marth, J. D., A genetic approach to mammalian glycan function. *Annu. Rev. Biochem.* **2003,** *72*, 643-691.
31. Stanley, P.; Ioffe, E., GLYCOSYLTRANSFERASE MUTANTS - KEY TO NEW INSIGHTS IN GLYCOBIOLOGY. *Faseb J.* **1995,** *9* (14), 1436-1444.
32. Ranjit, D. K.; Young, K. D., Colanic Acid Intermediates Prevent De Novo Shape Recovery of Escherichia coli Spheroplasts, Calling into Question Biological Roles Previously Attributed to Colanic Acid. *J Bacteriol* **2016,** *198* (8), 1230-40.
33. Laughlin, S. T.; Baskin, J. M.; Amacher, S. L.; Bertozzi, C. R., In vivo imaging of membrane-associated glycans in developing zebrafish. *Science* **2008,** *320* (5876), 664-667.
34. Gao, J. H.; Liao, J.; Yang, G. Y., CAAX-box protein, prenylation process and carcinogenesis. *Am. J. Transl. Res.* **2009,** *1* (3), 312-325.
35. Appels, N.; Beijnen, J. H.; Schellens, J. H. M., Development of farnesyl transferase inhibitors: A review. *Oncologist* **2005,** *10* (8), 565-578.
36. Troutman, J. M.; Erickson, K. M.; Scott, P. M.; Hazel, J. M.; Martinez, C. D.; Dodbele, S., Tuning the production of variable length, fluorescent polyisoprenoids using surfactant-controlled enzymatic synthesis. *Biochemistry* **2015,** *54* (18), 2817-27.
37. Henriksen, B. S.; Zahn, T. J.; Evanseck, J. D.; Firestine, S. M.; Gibbs, R. A., Computational and conformational evaluation of FTase alternative substrates: Insight into a novel enzyme binding pocket. *J. Chem Inf. Model.* **2005,** *45* (4), 1047-1052.
38. Lonhienne, T. G. A.; Sagulenko, E.; Webb, R. I.; Lee, K. C.; Franke, J.; Devos, D. P.; Nouwens, A.; Carrolla, B. J.; Fuerst, J. A., Endocytosis-like protein uptake in the bacterium Gemmata obscuriglobus. *Proc. Natl. Acad. Sci. U. S. A.* **2010,** *107* (29), 12883-12888.
39. Zhang, G.; Meredith, T. C.; Kahne, D., On the essentiality of lipopolysaccharide to Gram-negative bacteria. *Curr. Opin. Microbiol.* **2013,** *16* (6), 779-785.
40. Vaara, M., AGENTS THAT INCREASE THE PERMEABILITY OF THE OUTER-MEMBRANE. *Microbiol. Rev.* **1992,** *56* (3), 395-411.
41. Schindler, P. R. G.; Teuber, M., ACTION OF POLYMYXIN-B ON BACTERIAL-MEMBRANES - MORPHOLOGICAL CHANGES IN CYTOPLASM AND IN OUTER MEMBRANE OF SALMONELLA-TYPHIMURIUM AND ESCHERICHIA-COLI-B. *Antimicrobial Agents and Chemotherapy* **1975,** *8* (1), 95-104.
42. Kimura, Y.; Matsunaga, H.; Vaara, M., POLYMYXIN B-OCTAPEPTIDE AND POLYMYXIN B-HEPTAPEPTIDE ARE POTENT OUTER-MEMBRANE PERMEABILITY-INCREASING AGENTS. *J. Antibiot.* **1992,** *45* (5), 742-749.
43. Audia, J. P.; Winkler, H. H., Study of the five Rickettsia prowazekii proteins annotated as ATP/ADP translocases (Tlc): Only Tlc1 transports ATP/ADP, while Tlc4 and Tlc5 transport other ribonucleotides. *J. Bacteriol.* **2006,** *188* (17), 6261-6268.
44. Driscoll, T. P.; Verhoeve, V. I.; Guillotte, M. L.; Lehman, S. S.; Rennoll, S. A.; Beier-Sexton, M.; Rahman, M. S.; Azad, A. F.; Gillespie, J. J., Wholly Rickettsia! Reconstructed Metabolic Profile of the Quintessential Bacterial Parasite of Eukaryotic Cells. *mBio* **2017,** *8* (5), 27.
45. Varki, A., BIOLOGICAL ROLES OF OLIGOSACCHARIDES - ALL OF THE THEORIES ARE CORRECT. *Glycobiology* **1993,** *3* (2), 97-130.

46. Agard, N. J.; Prescher, J. A.; Bertozzi, C. R., A strain-promoted 3+2 azide-alkyne cycloaddition for covalent modification of biomolecules in living systems (vol 126, pg 15046, 2004). *J. Am. Chem. Soc.* **2005,** *127* (31), 11196-11196.
47. Troutman, J. M.; Subramanian, T.; Andres, D. A.; Spielmann, H. P., Selective modification of CaaX peptides with ortho-substituted anilinogeranyl lipids by protein farnesyl transferase: Competitive substrates and potent inhibitors from a library of farnesyl diphosphate analogues. *Biochemistry* **2007,** *46* (40), 11310-11321.
48. Dodbele, S.; Martinez, C. D.; Troutman, J. M., Species differences in alternative substrate utilization by the antibacterial target undecaprenyl pyrophosphate synthase. *Biochemistry* **2014,** *53* (30), 5042-50.
49. Troutman, J. M.; Sharma, S.; Erickson, K. M.; Martinez, C. D., Functional identification of a galactosyltransferase critical to Bacteroides fragilis Capsular Polysaccharide A biosynthesis. *Carbohydr Res* **2014,** *395*, 19-28.
50. Wiegand, I.; Hilpert, K.; Hancock, R. E. W., Agar and broth dilution methods to determine the minimal inhibitory concentration (MIC) of antimicrobial substances. *Nat. Protoc.* **2008,** *3* (2), 163-175.
51. Lambert, R. J. W.; Pearson, J., Susceptibility testing: accurate and reproducible minimum inhibitory concentration (MIC) and non-inhibitory concentration (NIC) values. *Journal of Applied Microbiology* **2000,** *88* (5), 784-790.
52. Bio-Rad, Quick Start™ Bradford Protein Assay Instruction Manual.
53. Farha, M. A.; Czarny, T. L.; Myers, C. L.; Worrall, L. J.; French, S.; Conrady, D. G.; Wang, Y.; Oldfield, E.; Strynadka, N. C. J.; Brown, E. D., Antagonism screen for inhibitors of bacterial cell wall biogenesis uncovers an inhibitor of undecaprenyl diphosphate synthase. *Proc. Natl. Acad. Sci. U. S. A.* **2015,** *112* (35), 11048-11053.
54. Duwe, A.; Rupar, C. A.; Horsman, G. B.; Vas, S. I., In Vitro Cytotoxicity and Antibiotic Activity of Polymyxin B Nonapeptide. *ANTIMICROBIAL AGENTS AND CHEMOTHERAPY* **1986,** *30* (2), 340-341.
55. Sawer, I. K.; Berry, M. I.; Ford, J. L., Effect of medium composition, agitation and the presence of EDTA on the antimicrobial activity of cryptolepine. *Lett. Appl. Microbiol.* **1997,** *25* (3), 207-211.
56. Tsubery, H.; Ofek, I.; Cohen, S.; Fridkin, M., Structure-function studies of polymyxin B nonapeptide: Implications to sensitization of gram-negative bacteria. *J. Med. Chem.* **2000,** *43* (16), 3085-3092.
57. Andrews, J. M., Determination of minimum inhibitory concentrations. *J. Antimicrob. Chemother.* **2001,** *48*, 5-16.
58. Comprehensive Natural Products II: Chemistry and Biology, Vol 9: Modern Methods in Natural Products Chemistry. *Comprehensive Natural Products Ii: Chemistry and Biology, Vol 9: Modern Methods in Natural Products Chemistry* **2010**, 1-769.
59. Tsang, P. H.; Li, G. L.; Brun, Y. V.; Ben Freund, L.; Tang, J. X., Adhesion of single bacterial cells in the micronewton range. *Proc. Natl. Acad. Sci. U. S. A.* **2006,** *103* (15), 5764-5768.
60. Toh, E.; Kurtz, H. D.; Brun, Y. V., Characterization of the Caulobacter crescentus Holdfast Polysaccharide Biosynthesis Pathway Reveals Significant Redundancy in the Initiating Glycosyltransferase and Polymerase Steps. *J. Bacteriol.* **2008,** *190* (21), 7219-7231.

61. Desai, J.; Wang, Y.; Wang, K.; Malwal, S. R.; Oldfield, E., Isoprenoid Biosynthesis Inhibitors Targeting Bacterial Cell Growth. *ChemMedChem* **2016,** *11* (19), 2205-2215.
62. Gisselberg, J. E.; Herrera, Z.; Orchard, L. M.; Llinas, M.; Yeh, E., Specific Inhibition of the Bifunctional Farnesyl/Geranylgeranyl Diphosphate Synthase in Malaria Parasites via a New Small-Molecule Binding Site. *Cell Chem. Biol.* **2018,** *25* (2), 185-+.
63. Fujisaki, S.; Ohnuma, S.; Horiuchi, T.; Takahashi, I.; Tsukui, S.; Nishimura, Y.; Nishino, T.; Kitabatake, M.; Inokuchi, H., Cloning of a gene from Escherichia coli that confers resistance to fosmidomycin as a consequence of amplification. *Gene* **1996,** *175* (1-2), 83-87.
64. Wang, C.; Yoon, S. H.; Shah, A. A.; Chung, Y. R.; Kim, J. Y.; Choi, E. S.; Keasling, J. D.; Kim, S. W., Farnesol Production From Escherichia coli by Harnessing the Exogenous Mevalonate Pathway. *Biotechnol. Bioeng.* **2010,** *107* (3), 421-429.
65. Ranjit, D. K.; Young, K. D., The Rcs stress response and accessory envelope proteins are required for de novo generation of cell shape in Escherichia coli. *J Bacteriol* **2013,** *195* (11), 2452-62.
66. Rohmer, M.; Grosdemange-Billiard, C.; Seemann, M.; Tritsch, D., Isoprenoid biosynthesis as a novel target for antibacterial and antiparasitic drugs. *Current opinion in investigational drugs (London, England : 2000)* **2004,** *5* (2), 154-62.
67. Lange, B. M.; Rujan, T.; Martin, W.; Croteau, R., Isoprenoid biosynthesis: The evolution of two ancient and distinct pathways across genomes. *Proc. Natl. Acad. Sci. U. S. A.* **2000,** *97* (24), 13172-13177.